Kinetic Isoforms of Intramembrane Charge in Intact Amphibian Striated Muscle

CHRISTOPHER L.-H. HUANG

From the Physiological Laboratory, University of Cambridge, Cambridge CB2 3EG, United Kingdom

ABSTRACT The effects of the ryanodine receptor (RyR) antagonists ryanodine and daunorubicin on the kinetic and steady-state properties of intramembrane charge were investigated in intact voltage-clamped frog skeletal muscle fibers under conditions that minimized time-dependent ionic currents. A hypothesis that RyR gating is allosterically coupled to configurational changes in dihydropyridine receptors (DHPRs) would predict that such interactions are reciprocal and that RyR modification should influence intramembrane charge. Both agents indeed modified the time course of charging transients at 100–200-μM concentrations. They independently abolished the delayed charging phases shown by q_γ currents, even in fibers held at fully polarized, −90-mV holding potentials; such waveforms are especially prominent in extracellular solutions containing gluconate. Charge movements consistently became exponential decays to stable baselines in the absence of intervening inward or other time-dependent currents. The steady-state charge transfers nevertheless remained equal through the ON and the OFF parts of test voltage steps. The charge–voltage function, $Q(V_T)$, shifted by ~+10 mV, particularly through those test potentials at which delayed q_γ currents normally took place but retained steepness factors ($k \approx 8.0$ to 10.6 mV) that indicated persistent, steeply voltage-dependent q_γ contributions. Furthermore, both RyR antagonists preserved the total charge, and its variation with holding potential, $Q_{max}(V_H)$, which also retained similarly high voltage sensitivities ($k \approx 7.0$ to 9.0 mV). RyR antagonists also preserved the separate identities of q_γ and q_β species, whether defined by their steady-state voltage dependence or inactivation or pharmacological properties. Thus, tetracaine (2 mM) reduced the available steady-state charge movement and gave shallow $Q(V_T)$ ($k \approx 14$ to 16 mV) and $Q_{max}(V_H)$ ($k \approx 14$ to 17 mV) curves characteristic of q_β charge. These features persisted with exposure to test agent. Finally, q_γ charge movements showed steep voltage dependences with both activation ($k \approx 4.0$ to 6.5 mV) and inactivation characteristics ($k \approx 4.3$ to 6.6 mV) distinct from those shown by the remaining q_β charge, whether isolated through differential tetracaine sensitivities, or the full approximation of charge–voltage data to the sum of two Boltzmann distributions. RyR modification thus specifically alters q_γ kinetics while preserving the separate identities of *steady-state* q_β and q_γ charge. These findings permit a mechanism by which transverse tubular voltage provides the primary driving force for configurational changes in DHPRs, which might produce q_γ charge movement. However, they attribute its kinetic complexities to the reciprocal allosteric coupling by which DHPR voltage sensors and RyR-Ca^{2+} release channels might interact even though these receptors reside in electrically distinct membranes. RyR modification then would still permit tubular voltage change to drive net q_γ charge transfer but would transform its complex waveforms into simple exponential decays.

INTRODUCTION

It is now generally accepted that charge movements are important in the control of sarcoplasmic reticular Ca^{2+} release by the transverse tubular potential in skeletal muscle (Schneider and Chandler, 1973). A step depolarization in a fully polarized intact fiber first elicits a rapidly rising q_β signal that then decays approximately exponentially. This is resistant to contractile inhibitors such as tetracaine or dantrolene sodium, and its voltage dependence is shallower (steepness factor, $k \approx 15$–20 mV) than that of most physiological processes regulated by membrane potential (Huang, 1982; Hui, 1983; Vergara and Caputo, 1982). Larger depolarizations close to contractile threshold voltages additionally elicit delayed "humps" attributed to a second q_γ charge localized selectively to the transverse tubules (Adrian and Peres, 1979; Huang and Peachey, 1989). These delayed waveforms became considerably faster and ultimately

Address correspondence to Christopher L.-H. Huang, Physiological Laboratory, Downing Street, Cambridge CB2 3EG, United Kingdom. Fax: 44-1-223-333840.

J. GEN. PHYSIOL. © The Rockefeller University Press • 0022-1295/96/04/515/20 $2.00
Volume 107 April 1996 515–534

indistinguishable from the remaining capacity transient, with larger depolarizations that nevertheless transferred increased steady-state charge (Huang, 1994*b*). Thus, their kinetic, steady-state, and pharmacological properties closely paralleled the steep voltage dependence shown by the release of intracellularly stored Ca^{2+} (Huang, 1981*a*, 1982, 1993; Hui, 1983; Vergara and Caputo, 1983; Hui and Chandler, 1990, 1991). It was suggested that this complex behavior reflects a cooperative transition (see, e.g., Huang, 1983) that involves feedback systems driven by the release of Ca^{2+} (an idea first suggested by Dr. W.K. Chandler, quoted in Horowicz and Schneider, 1981; see Csernoch et al., 1991; Pizarro et al., 1991). Alternatively, they could reflect intramembrane interactions involving the sensing units themselves (Huang, 1983, 1984; Hui and Chandler, 1990; Rios et al., 1993).

These two classes of scheme need not be mutually exclusive, but the latter suggestion was compatible with the architecture of the skeletal muscle triadic junction that suggested groupings of four dihydropyridine receptors (DHPRs; Rios and Brum, 1987; Huang, 1990) collectively coupled to a ryanodine receptor (RyR; review: Meissner, 1994; Franzini-Armstrong and Jorgensen, 1994). Thus the four DHPR particles in a tetrad might interact and thereby cooperatively alter their intrinsic rate constants (Huang, 1984; Rios et al., 1993) to generate complex q_γ currents under particular conditions. Alternatively, the entire charge might still relax but with a simple time course in states that precluded such interactions. Thus, Ca^{2+} release rates followed the fourth power of the charge movement $Q(t)^4$ when q_γ humps were absent in charge movements from cut fiber preparations that nevertheless demonstrated sarcoplasmic reticular Ca^{2+} release (Simon and Hill, 1992; Kovacs et al., 1979; Rakowski et al., 1985; Melzer et al., 1986). This suggested that Ca^{2+} release-channel opening required all four of its associated but otherwise independent charge movement particles to reach their activating configurations, whatever their kinetics. Hui and Chandler (1990, 1991) discussed situations in which q_γ currents that reflected cooperative rearrangements of groups of interacting DHPRs might interconvert to q_β currents that signaled the independent rearrangement of individual but otherwise identical receptors.

Complex q_γ currents appear specific to excitation–contraction coupling in skeletal muscle; this appears to involve direct allosteric interactions between tubular DHPR-voltage sensors and cisternal RyR-Ca^{2+} release channels (for a review see Huang, 1993). They do not contribute to the monotonically decaying Ca^{2+} channel gating currents in neurons (Kostyuk et al., 1981), arthropod skeletal muscle (Gilly and Scheuer, 1984), and mammalian cardiac muscle (Bean and Rios, 1989), even though all these systems are activated by elevations of cytosolic Ca^{2+}. However, the latter systems are differently triggered indirectly by extracellular Ca^2 entry (Beuckelman and Wier, 1988; Fabiato, 1985; Lopez-Lopez et al., 1995; Cannell et al., 1995; Sun et al., 1995). Such comparisons would associate complex q_γ charge movements specifically with the allosteric coupling proposed between tubular DHPRs and cisternal RyRs in skeletal muscle.

The present experiments test such an idea in intact fibers exposed to the gluconate-containing solutions known preferentially to reduce q_β relative to q_γ charge movements (Chen and Hui, 1991). This provided optimal conditions for the measurement of absolute quantities of steady-state charge and for the discrimination of q_γ charge with which comparisons could be drawn with other findings obtained in similar experimental solutions (Huang, 1994*a*, 1994*b*). They demonstrated that RyR modification by ryanodine and daunorubicin (see Discussion; for a review see Meissner, 1994) altered q_γ charge movements in a manner compatible with a reciprocal coupling between RyRs and the DHPRs in turn responsible for the observed charge transfers (Huang, 1990). Thus, the normally complex q_γ waveforms converted to simple exponential decays. Garcia et al. (1991) recently reported that ryanodine blocked delayed q_γ signals but also reduced ON charge movement while sparing OFF charge in cut fibers studied within a Vaseline gap. This differential effect on ON and OFF charges suggested that RyR antagonists blocked a release of intracellularly stored Ca^{2+}, which in turn provided the driving force for q_γ charge movement. The present studies reported instead that both ryanodine and daunorubicin preserved not only the total available charge but also its equality through the ON and OFF parts of applied voltage steps. Furthermore, they demonstrated that the q_β and q_γ charge species retained their separate identities as judged by their differential pharmacological sensitivities, steady-state voltage dependences, and inactivation characteristics.

METHODS

Sartorius muscles were dissected from cold-adapted frogs (*Rana temporaria*), which had been killed by concussion followed by decapitation and pithing, in Ringer solution at 4°C. The muscles were mounted in a temperature-controlled recording chamber and stretched to give fibers whose center sarcomere length was 2.2–2.4 μm as measured using an eyepiece graticule on a Zeiss Oberkochen (Germany) ×40 water immersion objective (Huang and Peachey, 1989). The bathing solution was then altered to an isotonic solution at the same temperature that consisted of 120 mM tetraethylammonium gluconate, 2.0 mM $MgCl_2$, 2.5 mM RbCl, 800 μM $CaCl_2$, 1.0 mM 3,4-diaminopyridine, 2×10^{-7} M tetrodotoxin, and 3 mM HEPES buffered to pH 7.0. It was then replaced by a similar solution to which 500 mM sucrose and either of the test agents, ryanodine (Penick Corp, Lyndhurst, NJ,

lot 704-RWP no. 2; a kind gift of Dr. John Sutko) or daunorubicin (Sigma Chemical Co., St. Louis, MO), at concentrations of 0 (controls), 100, or 200 μM were added. The electrophysiological studies that followed were similarly conducted in cooled (2–4°C) preparations within an interval of 30 min to 2 h of introducing these experimental solutions.

The pelvic ends of superficial muscle fibers directly exposed to the bathing solution were subjected to a three-microelectrode voltage clamp that used conventional 3–5 MΩ glass electrodes. The voltage-recording electrodes, filled with 3M KCl, were positioned at distances of l = 375 μm (voltage control electrode, V_1) and $2l$ = 750 μm (second voltage electrode, V_2) from the fiber end, respectively. The current injection electrode I_0, filled with 2M K citrate, was positioned at $5l/2$ = 940 μm. It was held by a shielded electrode holder designed and built around a 50-Ω SMB gold-plated coaxial cable assembly (Radio Spares, Corby, UK) by B. Secker. Signals that represented the clamp voltage V_1, the voltage drop ($V_1 - V_2$), and the injected current $I_0(t)$ were filtered through three-pole Butterworth filters set to a cut-off frequency of 1.0 kHz and then sampled using a PDP 11/23 computer (Digital Equipment Corp., Marlboro, MA) with a model 502 interface (Cambridge Electronic Design, Cambridge, UK). They were acquired through 12-bit analogue-to-digital conversion at a sampling interval of 200 μs. Five sweeps, spaced by intervals of 20 s, were averaged into each test or control record when measuring steady-state charge.

The experiments sought to measure absolute quantities of nonlinear intramembrane charge and therefore required stable control records with which to compare the test transients to derive the nonlinear charge movement. Control pulse procedures that used the standard pulse length of 124 ms accordingly regularly bracketed successive sets of all test runs. Cable constants calculated from the successive control traces were assessed for significant systematic changes in fiber stability and condition over time. The figure legends list the linear cable constants obtained from those control sweeps that preceded and followed the experimental runs. Steady-state values of $V_1(t)$, $V_2(t)$, and the injected current $I_0(t)$ were achieved well before the end of the depolarizing control steps. The latter returned the membrane potential to the −90-mV prepulse potential 500 ms after application of prepulses to −120 mV. These steady levels could be determined directly from the traces without the sloping baseline corrections required for both control and test responses in cut fiber preparations (Melzer et al., 1986). It was further possible to assess fiber condition and stability in the intact preparations through computations of length constants, λ, internal longitudinal resistances, r_i, and membrane resistances of unit fiber length, r_m. Calculation of fiber diameters, d, and specific membrane resistances, R_m, assumed an internal sarcoplasmic resistivity, R_i, of 391 Ω cm in 2.5 times hypertonic solution at 2°C, and a temperature coefficient of 0.73 (Hodgkin and Nakajima, 1972); these calculations were performed for each individual average. In contrast, such values of r_m and R_m could not be unambiguously determined in cut fibers studied between Vaseline seals, owing to current shunts beneath the seals (Chandler and Hui, 1990). The latter configuration also requires corrections for the transient currents, up to one-third of which actually traverse plasma membrane beneath the seals or pass directly from the current passing end-pool to the central pool. Such corrections assume that the ratios of the internal longitudinal and the shunt resistances remain constant throughout the duration of the experiment. In the present studies, the membrane current as a function of time t through unit fiber surface area, $I_m(t)$, was calculated from the equation

$$I_m(t) = [V_1(t) - V_2(t)]\, d/(6l^2 R_i).$$

The pulse procedures intercalated control voltage steps between sets of three to four test runs. This made it possible to monitor fiber stability as reflected in computed values of cable constants and DC currents.

Additional controls assessed for effects of tubular attenuations that would alter the effective tubular length constant λ_T and therefore the overall specific membrane resistance R_m in the solutions that contained the test reagents. Such tubular effects would influence the measurements of effective charge. They were assessed by calculating the limiting ratio, h, between the effective capacitance, C_{eff}, and the total available charge, C_∞. This was determined from experimental values of the fiber diameters, a, and specific membrane resistances, R_m, derived from full cable analyses of both test and control records. The computed values of the fiber cable constants were introduced into a distributed lattice model for the transverse tubules in which the fraction of fiber volume occupied by the tubules was $\rho = 3 \times 10^{-3}$, the volume/surface ratio of the tubules was $\zeta = 10^{-6}$ cm, the tubular network factor was $\sigma = 0.5$ (Peachey, 1965), and the tubular luminal conductivity was $G_L = 10^{-2}$ S cm^{-1}. This gave a tubular membrane capacitance of unit fiber volume of $C^*_w = C_w\rho/\zeta$ and an effective tubular linear radial conductivity of $G^*_L = G_L\rho$. It was assumed that the specific membrane capacitance of both tubular, C_w, and surface, C_s, membrane was 1.0 μF cm^{-2}. The following transcendental equation then related the overall membrane admittance referred to unit surface area of muscle fiber to the cable properties of the surface and tubular membrane (see Adrian et al., 1969; Huang, 1981*b*):

$$1/R_m = G_s + G^*_L I_1(a/\lambda_T)/\lambda_T I_0(a/\lambda_T).$$

The above equation was solved numerically by Newton–Raephson iteration for the limiting (worst) case that attributed the entire fiber leak conductance to transverse tubular as opposed to surface membrane, for which the surface conductance $G_s = 0$. The resulting values of the zeroth and first-order modified Bessel functions $I_0(a/\lambda_T)$ and $I_1(a/\lambda_T)$ were evaluated by standard converging series expansions. This yielded values of the ratio $I^*(a/\lambda_T) = I_1(a/\lambda_T)/I_0(a/\lambda_T)$ from which the limiting value of h at the corresponding test or control membrane potential was calculated:

$$h \geq (1/C_\infty)\left\{C_s + (aC^*_w/2)\left[1 - \{I^*(a/\lambda_T)\}^2\right]\right\}.$$

The C_∞ term was determined from the limiting values that correspond to uniform tubular polarization: $h = 1$ and $\lambda_T = \infty$. The values of h calculated from the experimental values of R_m and a from both bracketing control and test voltages confirmed that the tubular cable attenuations reduced net charge transfer by <1–2% in the particular experimental solutions adopted here and thus excluded significant variations in the limiting value of h with test voltage. The present studies therefore effectively measured the entire available intramembrane charge within both surface and tubular membrane at all the test and control voltages that were investigated.

Studies of the inactivation properties of the intramembrane charge adopted similar precautions. Their control protocols were imposed at least 30 s after the fiber was returned to a fully polarized holding potential of −90 mV. These both preceded and bracketed successive sets of test runs. Again, the control pulse procedures superimposed +30-mV steps at intervals of 500 ms after prepulse steps to −120 mV. The test voltage steps then were applied at least 60 s after shifts to the specific holding potential, V_H, being investigated. They involved a return of the membrane potential to a fixed prepulse level of −90 mV, followed by a fixed test step to −20 mV. The membrane potential was then returned to the holding level under study after the "off" of the current response. Each test or control record was the average of five such sweeps.

Charge movements were derived from simple comparisons of test traces, with control currents appropriately scaled to the ratio of the amplitudes of the test to the control voltage steps. The same scaling and subtraction were also applied to averaged records of the test and the control voltage steps that were recorded from the voltage clamp (V_1) electrode. The latter subtractions verified that the derived charge movements indeed reflected nonlinear contributions to the observed electrical behavior of the fibers examined. To further correct for small changes in linear membrane properties through the course of each set of test voltage steps, the control records with which the comparisons were made were constituted from a weighted mean of the two bracketing control records, with the relative weighting determined by the position of the relevant test response within the bracketed test sequence. All the results of the calculations outlined here are expressed as means ± SEM.

The steady-state charge–voltage data were described in terms of Boltzmann functions that related the charge movement, $Q(V)$, to the maximum charge, Q_{max}, the transition voltage, V^*, and the steepness factor, k. Thus,

$$Q(V) = Q_{max}/\{1 + \exp[-(V - V^*)/k]\}.$$

Some of the data were amenable to fitting to the sum of two rather than one Boltzmann function as described by Hui and Chandler (1990):

$$\Sigma Q(V) = Q_\beta(V) + Q_\gamma(V).$$

The inactivation functions were also empirically described by two-state Boltzmann-type functions and made use of the values of the charge $Q_{-20}(V_H)$ transferred by a voltage step from −90 to −20 mV:

$$Q_{-20}(V_H) = Q_{max,-20}\{1 - 1/\{1 + \exp[-(V_H - V_H^*)/k]\}\}.$$

All such functions were optimized by a Levenberg–Marquadt procedure (Press et al., 1986) that performed successive least-squares minimizations for the values of each of the parameters a_j of a generalized nonlinear function $y(x)$. This was computed simultaneously over all the experimentally obtained mean values $y(x_i)$ that were obtained at each ith test voltage x_i. Successive iterations therefore sought to minimize the values of χ_v^2 in the weighted fit derived from the mean and standard errors of the data points y_i:

$$\chi_v^2 = \Sigma\{[y_i - y(x_i)]^2/(\sigma_i^2 v)\}.$$

The number of degrees of freedom, v, incorporates not only the number of data points, n, but also the number of variables, N, by the relationship

$$v = n - N - 1.$$

The curve fits used a weighting factor for each point, w_i, that was determined by the inverse of its variance, σ_i^2, in turn normalized to the average of all such weighting factors. This precaution yielded the maximum likelihood that the fitted function would represent the distribution of the parent data.

RESULTS

Effective Conditions for Antagonist Action

The experiments first sought conditions that reproducibly converted q_γ charge movements from a form that showed complex "hump" kinetics at threshold voltages to one that consistently generated monotonic decays. They empirically demonstrated that both of the RyR agents ryanodine and daunorubicin independently achieved this effect under appropriate conditions. Previous studies that applied ryanodine (0.02–500 μM) to intact amphibian fibers obtained viable experimental preparations with 500 μM reagent in fibers in normal Ringer and with 10 μM ryanodine in fibers in isotonic tetraethylammonium chloride–containing solutions at room temperature. Such conditions yielded normal charge–voltage curves but only permitted investigation of subthreshold test voltages and not of more depolarized potentials through which most charge movement takes place. However, the addition of even 0.02 μM ryanodine initiated irreversible contractures in cooled (5°C) fibers exposed to moderately hypertonic (350 mM sucrose) tetraethylammonium chloride–containing solutions in both amphibian (Baylor et al., 1989) and mammalian (Fryer et al., 1989) muscle.

The present studies employed higher (100–200 μM) ryanodine concentrations, and exposed fibers to further elevated extracellular tonicities (500 mM sucrose) under consistently cooled conditions. This gave viable and stable preparations amenable to electrophysiological study, as confirmed in the linear cable analyses of the control pulses regularly intercalated through successive test procedures. This analysis thus excluded significant changes in linear effective capacitance in fibers of comparable diameter after applications of test agent. This contrasts with earlier reports that tetracaine reduced linear capacitance by 30–40% in fibers studied in a Vaseline gap (Garcia et al., 1991). The chosen conditions were then also adopted both in the control studies and the experiments that applied daunorubicin instead of ryanodine to ensure comparable and fully controlled conditions throughout.

In addition to studying transients, the experiments characterized steady-state charge–voltage curves and in-

activation properties in control fibers and preparations exposed to the test agents. This also required unambiguous determinations of cable constants, which are possible in intact fiber preparations, both to follow fiber stability through the experimental runs and to exclude significant tubular attenuations. This was not entirely possible in cut fibers (Garcia et al., 1991). Finally, the cable constants of treated and untreated muscle fiber groups were matched to permit comparisons against diameter and linear membrane capacitance. This made it possible additionally to assess the conservation (or otherwise) and properties of steady-state charge through the experimental maneuvers and the extent to which the q_β and q_γ charge movements retained their distinct identities even after antagonist modification of q_γ kinetics.

Small Shifts in the Charge–Voltage Curve Produced by Ryanodine Receptor Antagonists

Fig. 1 *A* displays charge movements from intact fibers in response to progressively increasing depolarizing test voltage steps made from the −90-mV holding potential in the absence of either ryanodine or daunorubicin. The bracketing control transients were obtained at a membrane potential of −90 mV both at the outset [e.g., Fig. 1 *B* (*a*)] and following [Fig. 1 *B* (*b*)] all the experimental runs and then compared to assess prepa-

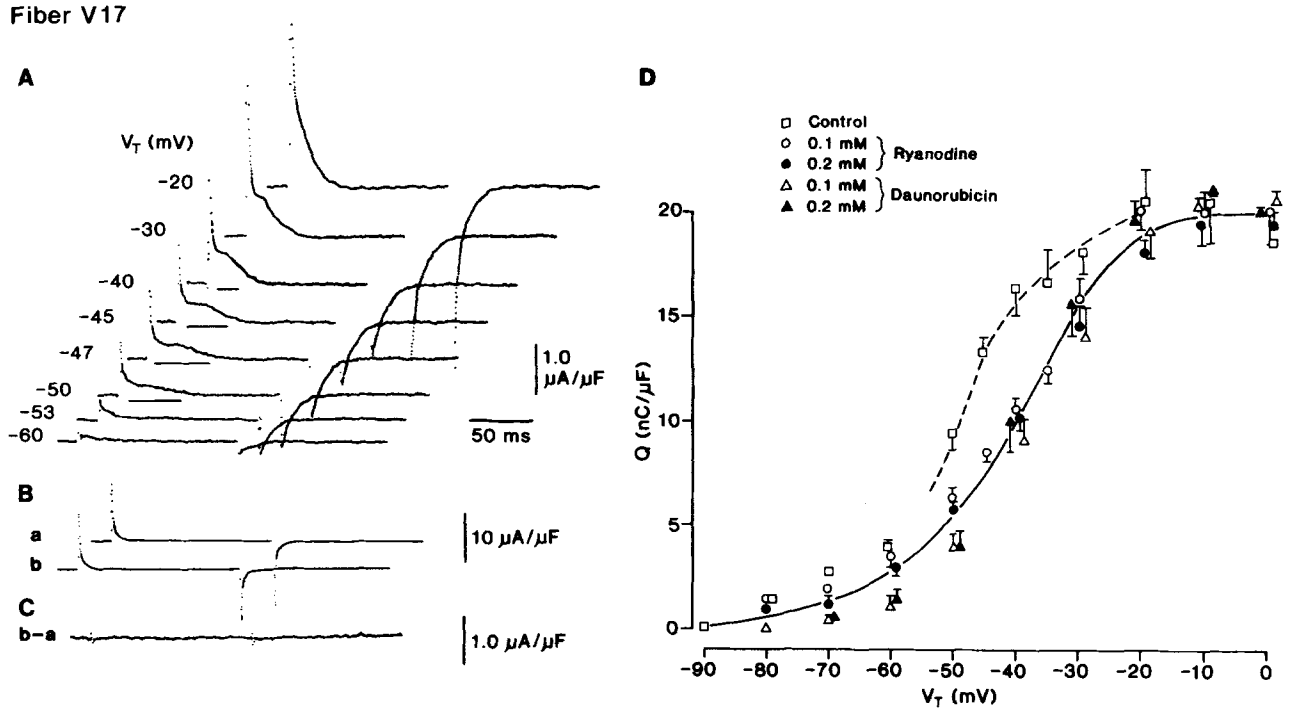

FIGURE 1. Ryanodine receptor antagonists shift the voltage dependence of nonlinear charge over voltages normally associated with q_γ currents. (*A*) Charge movements obtained in response to voltage steps to progressively more depolarized test potentials, V_T, from a −90 mV holding potential in fibers exposed to gluconate-containing solutions, in the absence of test reagents. (*B*) Plots of total capacity transients obtained at the −90-mV control voltage (*a*) before and (*b*) after the test runs. (*C*) The difference (*b* − *a*) demonstrates an absence of significant electrical changes at the beginning and the end of each run. (*D*) Charge–voltage relationships obtained in the absence of test reagents (*open squares*) and in the presence of 100 μM (*open triangles*) and 200 μM (*filled triangles*) daunorubicin, and 100 μM (*open circles*) and 200 μM (*filled circles*) ryanodine. Curves drawn by eye. (*A*) Fiber V17: temperature = 3.8°C; R_i = 373 Ω cm. Initial cable constants: λ = 1.76 mm; r_i = 7436 kΩ cm^{-1}; diameter = 80 μm; r_m = 227 kΩ cm; R_m = 5.7 kΩ cm^2; C_m = 5.5 μF cm^{-2}. Final cable constants: λ = 1.8 mm; r_i = 8,296 kΩ cm^{-1}; diameter = 81 μm; r_m = 285 kΩ cm; R_m = 6.8 kΩ cm^2; C_m = 5.9 μF cm^{-2}. (*D*) Seven control fibers studied in the absence of test agents: temperature = 2.9 ± 0.31°C; R_i = 407.6 ± 5.7 Ω cm. Initial cable constants: λ = 1.9 ± 0.35 mm; r_i = 12,265 ± 2,077 kΩ cm^{-1}; diameter = 71.0 ± 6.86 μm; r_m = 386.3 ± 72.5 kΩ cm; R_m = 8.82 ± 2.62 kΩ cm^2; C_m = 6.82 ± 0.39 μF cm^{-2}. Final cable constants: λ = 1.84 ± 0.33 mm; r_i = 11,617 ± 2,142 kΩ cm^{-1}; diameter = 72.9 ± 6.7 μm; r_m = 323.8 ± 65.6 kΩ cm; R_m = 8.13 ± 2.41 kΩ cm^2; C_m =7.96 ± 0.60 μF cm^{-2}. Four fibers studied in 100 μM ryanodine: temperature = 4.2 ± 0.01°C; R_i = 407.6 ± 1.56 Ω cm. Initial cable constants: λ = 1.46 ± 0.1 mm; r_i = 14,253 ± 3,609 kΩ cm^{-1}; diameter = 65.4 ± 6.8 μm; r_m = 274.4 ± 28.9 kΩ cm; R_m = 5.41 ± 0.35 kΩ cm^2; C_m = 9.61 ± 2.37 μF cm^{-2}. Final cable constants: λ = 1.29 ± 0.04 mm; r_i = 14,219 ± 3,064 kΩ cm^{-1}; diameter = 64.7 ± 6.9 μm; r_m = 225.4 ± 33.02 kΩ cm; R_m = 4.30 ± 0.18 kΩ cm^2; C_m = 10.3 ± 2.3 μF cm^{-2}. Six fibers studied in 100 μM daunorubicin: temperature = 3.4 ± 0.3°C; R_i = 418 ± 3.6 Ω cm. Initial cable constants: λ = 1.5 ± 0.17 mm; r_i = 9,586 ± 1,072 kΩ cm^{-1}; diameter = 76.8 ± 4.7 μm; r_m = 208.9 ± 37.4 kΩ cm; R_m = 4.97 ± 1.00 kΩ cm^2; C_m = 9.53 ± 1.63 μF cm^{-2}. Final cable constants: λ = 1.2 ± 0.08 mm; r_i = 9,376 ± 1,225 kΩ cm^{-1}; diameter = 78.2 ± 5.12 μm; r_m = 133.3 ± 24.0 kΩ cm; R_m = 3.1 ± 0.43 kΩ cm^2; C_m = 11.42 ± 1.84 μF cm^{-2}.

ration condition and stability through the test procedures. Fig. 1 *C* thus confirms an essentially null difference between (*b*) and (*a*). The figure legends additionally provide full cable analyses of such bracketing control records. Several further measures also enhanced charge separation and the reliable measurement of steady-state charge at the test potentials. Thus, use of the impermeant anion substitute gluconate minimized Cl^- conductances and therefore the standing currents required both to shift holding potentials and to maintain test potentials. It also provided records that emphasized the distinction between q_β and q_γ charge movement (cf. Chen and Hui, 1991; Huang 1994*a*, 1994*b*; see Introduction). Finally, the substantial replacement of external Ca^{2+} by Mg^{2+} suppressed Ca^{2+} currents, and the inclusion of 3,4-diaminopyridine as well as tetraethylammonium ions suppressed K^+ currents.

All charge movements decayed in the absence of inward current or oscillatory phases to stable baselines under these conditions (cf. Huang, 1994*a*, *b*; Shirokova et al., 1994) with ON currents consistently outward and OFF currents inward in direction. The final steady current slopes for both the ON and the OFF responses were everywhere less than 0.0007 μA $(\mu F\ ms)^{-1}$ and did not vary significantly with test potential. Thus, corrections previously required for sloping current baselines in both control and test responses in some cut fiber preparations (Melzer et al., 1986) and in test records in intact preparations (Huang and Peachey, 1989) proved unnecessary. This expedited reproducible integrations of transients to derive steady-state charge.

Both ON and OFF charge movements in response to the depolarizing and repolarizing phases of the test steps consisted of simple exponential q_β decays that progressively increased with test depolarizations more negative than −50 mV. Larger ON depolarizing steps also elicited additional, delayed q_γ, current contributions that became prominent by test voltages around −47 mV. These were prolonged over 50 ms at such threshold potentials and were particularly marked in gluconate-containing solutions. This confirmed earlier reports that chloride replacement by extracellular gluconate enhanced visualization of the q_γ charge movement by preferentially suppressing q_β charge (Chen and Hui, 1991; Huang, 1994*a*). The q_γ charge movements thus were distinguishable from the early q_β decays through a substantially wider voltage range, −50 to −30 mV, than in fibers in sulfate-containing bathing solutions (Huang, 1982). As reported on earlier occasions, their form and amplitude varied steeply with test voltage. Even a 3–5-mV further depolarization from their −50-mV threshold made them considerably larger and more rapid. Still larger test steps merged the q_γ humps with the q_β decays.

Control charge–voltage curves (Fig. 1 *D*: *squares*; means ± SEM) from fibers before addition of RyR antagonists closely agreed with earlier findings under similar conditions (Hui and Chandler, 1990; Huang, 1994*a*). The intramembrane charge gradually increased with small depolarizations from the −90-mV reference level but then rose sharply at test voltages around −50 mV coincident with the appearance of q_γ humps. Still larger voltage steps next produced a more gradual increase to a maximum charge of 20 ± 2.2 nC μF^{-1}. This is less than values of 28–30 nC μF^{-1} usually reported in intact fibers exposed to sulfate (Huang, 1982; Hui, 1983) but agrees with earlier reports in both cut (Chen and Hui, 1991) and intact fibers exposed to gluconate (Huang, 1994*a*). Thus, the overall form of the charge–voltage curves obtained from fibers in gluconate-containing solutions in the absence of RyR antagonists deviated significantly from the expectations of a two-state single Boltzmann system.

Fig. 1 *D* also plots steady-state charge–voltage curves for fibers treated with ryanodine (100 or 200 μM: *open circles* and *filled circles*, respectively) or daunorubicin (100 or 200 μM; *open triangles* and *filled triangles*, respectively). The charge voltage curves $Q(V_T)$ shifted in the positive direction, particularly over test potentials between −50 to −30 mV, where the delayed q_γ currents were normally observed in control solutions. However, the plots retained similar values of maximum charge, Q_{max}. The latter value was reached at much the same depolarizing voltages between −20 and 0 mV. The charge–voltage plots also altered to a form that more closely resembled a single Boltzmann plot than did the control results obtained in the absence of RyR antagonists. Accordingly, the primary aim of the analysis in Table I was simply to draw overall comparisons with earlier results in cut fibers in the same solutions (Jong et al., 1995). Thus, Table I displays the results of least-squares minimizations of the findings in Fig. 1 *D* to single Boltzmann distributions with the maximum charge, Q_{max}, transition voltage, V^*, and steepness factor, k, left as free parameters. The steepness factors ($k \approx 8$ mV) and transition voltages ($V^* \approx -50$ mV) closely agreed with recent values from cut fibers in similar extracellular solutions ($k \approx 7$ mV and $V^* \approx -48$ mV in Table II of Jong et al., 1995) when test agents were absent. This marked voltage dependence was attributed to steady-state contributions from a distinct species of q_γ charge in both intact (Adrian and Peres, 1979; Huang, 1982; Hui, 1983) and cut (Hui and Chandler, 1990, 1991) muscle fibers in this recent work (Jong et al., 1995). It contrasts with the more gradual variations ($k \approx 14$ to 15 mV; see Table IV below) attributed to the q_β charge.

Table I also indicates that ryanodine and daunorubicin consistently shifted the transition potential, V^*, by +10 mV from around −50 to −40 mV. However, they preserved the maximum charge, Q_{max}, at ~20 nC μF^{-1}

TABLE I

Analysis of Charge–Voltage Curves Q(V) from Fibers Studied in the Presence and Absence of 100 or 200 μM Ryanodine or Daunorubicin

Experimental condition	Number of fibers (n)	Maximum charge Q_{max} (nC μF^{-1})	Transition potential V^*(mV)	Steepness factor k (mV)
Control:				
0 μM ryanodine				
0 μM daunorubicin	7	19.25 ± 0.53	−50.5 ± 1.12	8.0 ± 1.03
100 μM ryanodine				
0 μM daunorubicin	4	20.01 ± 0.37	−39.0 ± 1.41	9.5 ± 1.29
200 μM ryanodine				
0 μM daunorubicin	5	20.18 ± 1.00	−40.1 ± 1.96	10.6 ± 1.53
0 μM ryanodine				
100 μM daunorubicin	6	18.56 ± 0.78	−38.7 ± 1.53	7.7 ± 1.25
0 μM ryanodine				
200 μM daunorubicin	4	21.21 ± 0.84	−37.3 ± 1.41	8.0 ± 1.14

Least-squares determinations of maximum charge, Q_{max}, transition voltage, V^*, and slope factor, k (given as means ± SEM), in a single Boltzmann function given by $Q(V) = Q_{max}/\{1 + \exp[-(V-V^*)/k]\}$ for n fibers in each case. Fibers studied in the absence of tetracaine.

(with standard errors largely <1.0 nC μF^{-1}). Ryanodine did increase (to $k \approx$ 9–10 mV), although daunorubicin slightly decreased the steepness factors (to $k \approx$ 7–8 mV). These values nevertheless more closely suggested the persistence of contributions from a steeply voltage-dependent q_γ charge than they did a transformation of the entire charge into the q_β species, with its larger steepness factors ($k \approx$ 14 to 15 mV; see Table IV below). However, as there was a change in the shape of the charge–voltage curve after addition of RyR antagonists, it may not be entirely appropriate to make detailed comparisons of slope factors derived from fits to a single Boltzmann function. Therefore, more detailed studies that included assessments of the individual q_β and q_γ charge species were also performed (see Table VI).

Table II extends the minimization procedures to the sum of two rather than one Boltzmann function (cf. Hui and Chandler, 1990). Values of maximum charge, Q_{max}, transition voltage, V^*, and steepness factor, k, in fibers spared RyR antagonist action then agreed with earlier determinations for q_β and q_γ charge (Hui and Chandler, 1990) apart from the diminished q_β charge expected in the presence of gluconate (cf. Chen and Hui, 1991). These values additionally confirmed the pharmacological analyses described below (cf. Hui and Chen, 1992). When applied to data from fibers exposed to RyR antagonists, the successive iterations yielded progressively diminishing values of one of the Q_{max} terms, increasingly positive values of its corresponding transition potential, V^*, and increasing values of the standard error of the slope factor k. This resembles recent reports for gluconate-containing solutions (Jong et al., 1995), the similar convergences of which toward single Boltzmann functions were attributed to the smaller proportion of q_β charge or closer values of V^* shown by q_β and q_γ in gluconate-treated fibers. The latter was confirmed in the pharmacological analysis below; this would lead to convergences to a single Boltzmann function whose value of k fell between those of q_β and q_γ, respectively.

Finally, Table I confirms that the chosen test reagent concentrations accomplished their maximal effect on the steady-state charge. Thus, doubling the concentration of either ryanodine or daunorubicin from 100 to 200 μM did not produce significantly larger effects on the charge–voltage relationship. Nevertheless, the

TABLE II

Analysis of Charge Voltage Curves Q(V) from Fibers Studied in the Absence of Both Ryanodine and Daunorubicin

Charge species (in 0 μM ryanodine; 0 μM daunorubicin)	Number of fibers (n)	Maximum charge Q_{max} (nC μF^{-1})	Transition potential V^* (mV)	Steepness factor k (mV)
q_β	7	10.18 ± 1.01	−39.8 ± 2.34	19.04 ± 1.37
q_γ	7	10.88 ± 0.75	−51.4 ± 1.05	3.6 ± 0.67

Least-squares minimizations for the determination of maximum charge, Q_{max}, transition voltage, V^*, and slope factor, k (given as means ± SEM), in each of two Boltzmann terms $\Sigma Q(V) = Q_\beta(V) + Q_\gamma(V)$, where each term is given by an equation of the form $Q(V) = Q_{max}/\{1 + \exp[-(V-V^*)/k]\}$ for n fibers in each case, as described in Hui and Chandler (1990). Fibers in tetracaine-free solutions.

higher concentration (200 μM) of either agent was used in all of the studies that follow.

Monotonic Charging Decays in Daunorubicin and Ryanodine

Figs. 2 *A* and 3 *A* display charge movements from fully polarized fibers exposed, respectively, to 200 μM ryanodine and daunorubicin in gluconate-containing solutions. The depolarizing test steps explored the entire range of potentials between −80 and 0 mV in progressive 5 mV increments. Both test agents independently produced similar and noticeable effects. Thus, both the ON and OFF charge movements now consisted exclusively of monotonic decays that increased with the size of the test voltage excursion until charge saturation. There were no obvious delayed q_γ components, even at relatively high display gains. In this respect, the charge movements now resembled the exponential transients previously reported in some cut fiber preparations (Melzer et al., 1986; Rakowski et al., 1985), as opposed to the complex waveforms reported in intact fiber preparations at certain voltages (Adrian and Peres, 1979; Huang, 1982). Both ON and OFF responses decayed completely to leave unambiguous DC baselines with insignificant slopes everywhere $< \pm$ 0.0004 μA (μF ms)$^{-1}$ (n = 5 fibers in the presence of ryanodine, and n = 4 fibers in the presence of daunorubicin, respectively) at all the test voltages examined. The kinetic features such as dips or late time-dependent currents that have been reported elsewhere were absent (cf. Garcia et al., 1991; Pizarro et al., 1991; Csernoch et al., 1991).

These findings prompted experiments that explored two major explanations for this antagonist action. Thus, ryanodine and daunorubicin might simply abolish a (q_γ) fraction of steady-state charge in an effect identical to that of tetracaine (cf. Huang, 1982; Hui, 1983; Vergara and Caputo, 1982). This possibility has been raised earlier. It would predict a reduction in maximum charge Q_{max} (Garcia et al., 1991). Alternatively, the total available charge may be conserved but its kinetics could still be altered. This possibility would predict that maximum overall charge would be conserved.

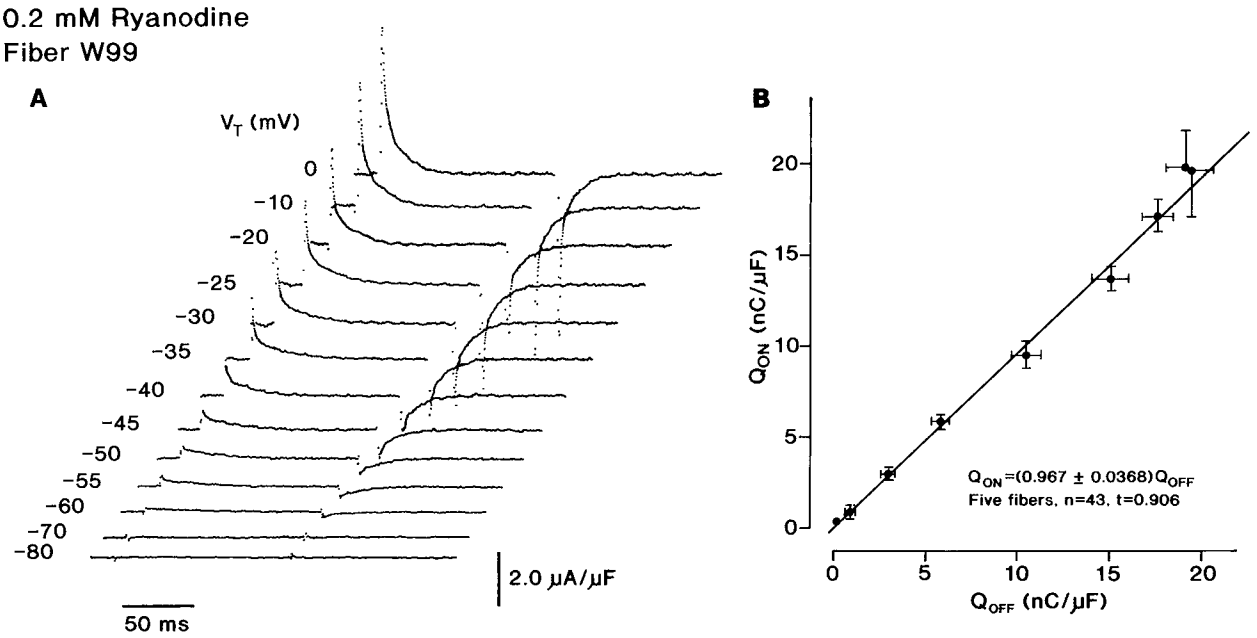

FIGURE 2. Charge movements in the presence of 200 μM ryanodine. (*A*) Charge movements obtained in response to test voltage steps from the holding potential of −90 mV to a range of closely incremented test voltages V_T. (*B*) The leak admittance corrections obtained from the DC estimations based on the last 40 ms of the ON currents and the last 80 ms of the OFF response in both test and control records yielded the capacity component of the current, which could be integrated to give ON plotted against OFF values that fell close to a straight line of equality through the origin. (*A*) Fiber W99: temperature = 4.1°C; R_i = 408.8 Ω cm. Initial cable contants: λ = 3.7 mm; r_i = 4,566 kΩ cm^{-1}; diameter = 106.7 μm; r_m = 617.0 kΩ cm; R_m = 20.6 kΩ cm^2; C_m = 10.6 μF cm^{-2}. Final cable constants: λ = 3.6 mm; r_i = 4,111.8 kΩ cm^{-1}; diameter = 112.5 μm; r_m = 554.6 kΩ cm; R_m = 19.61 kΩ cm^2; C_m = 11.32 μF cm^{-2}. (*B*) Five fibers studied in 200 μM ryanodine: temperature = 3.8 ± 0.13°C; R_i = 413 ± 1.7 Ω cm; Initial cable constants: λ = 2.6 ± 0.34 mm; r_i = 8,204 ± 2,869 kΩ cm^{-1}; diameter = 92.5 ± 9.8 μm; r_m = 430.3 ± 42.5 kΩ cm; R_m = 12.4 ± 2.16 kΩ cm^2; C_m = 8.5 ± 1.02 μF cm^{-2}. Final cable constants: λ = 2.5 ± 0.38 mm; r_i = 8,366 ± 3,031 kΩ cm^{-1}; diameter = 92.7 ± 10.2 μm; r_m = 371.3 ± 54.6 kΩ cm; R_m = 11.12 ± 2.39 kΩ cm^2; C_m = 9.04 ± 1.12 μF cm^{-2}.

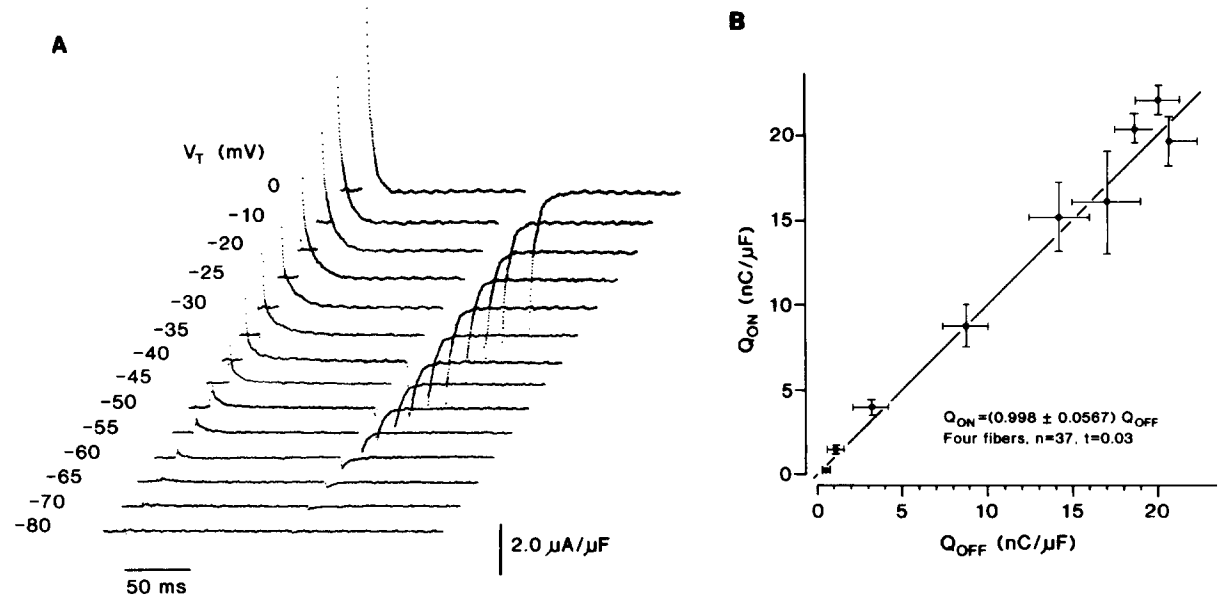

FIGURE 3. Charge movements in the presence of 200 μM daunorubicin. (*A*) Charge movements obtained in response to test voltage steps from the holding potential of −90 mV to a range of closely incremented test voltages V_T. (*B*) ON charge plotted against OFF charge. (*A*) Fiber W88: temperature = 4.0°C; R_i = 410 Ω cm. Initial cable constants: λ = 1.4 mm; r_i = 10,586 kΩ cm^{-1}; diameter = 70.0 μm; r_m = 199.4 kΩ cm; R_m = 4.37 kΩ cm^2; C_m = 9.0 μF cm^{-2}. Final cable constants: λ = 1.12 mm; r_i = 10,270 kΩ cm^{-1}; diameter = 70.7 μm; r_m = 1,295 kΩ cm; R_m = 2.87 kΩ cm^2; C_m = 9.8 μF cm^{-2}. (*B*) Four fibers studied in 200 μM daunorubicin: temperature = 4.3 ± 0.49°C; R_i = 407 ± 6.3 Ω cm. Initial cable constants: λ = 2.1 ± 0.16 mm; r_i = 7,870 ± 1639 kΩ cm^{-1}; diameter = 86.5 ± 8.9 μm; r_m = 308.7 ± 27.2 kΩ cm; R_m = 8.17 ± 0.57 kΩ cm^2; C_m = 9.03 ± 1.23 μF cm^{-2}. Final cable constants: λ = 2.09 ± 0.17 mm; r_i = 6,814 ± 890 kΩ cm^{-1}; diameter = 89.8 ± 6.74 μm; r_m = 287.4 ± 33.6 kΩ cm; R_m = 8.10 ± 1.00 kΩ cm^2; C_m = 9.96 ± 1.04 μF cm^{-2}.

Persistence of ON–OFF Charge Equality in Ryanodine and Daunorubicin

The first conservation tests simply compared integrated ON and OFF charge movements obtained in the presence of either ryanodine or daunorubicin. Individual test and control (V_1 − V_2) records were integrated using Simpson's rule after subtraction of the template derived from scaling of the applied voltage excursion by its ratio with the final steady-state leak current (see Huang, 1994*a*; Hui and Chandler 1991). This precaution excluded artefactual ionic current contributions to the leak currents introduced by variations in the waveform of the test, the control voltage clamp steps, or both. Such contributions would introduce errors into the integrations of uncorrected difference (charge movement) traces. The net charge movement was then determined by comparison of the test and control integration records while monitoring the running integrals of nonlinear charge and verifying that these running integrals converged to a steady level with time.

Figs. 2 *B* and 3 *B* compare the values of ON and OFF charge obtained in fibers exposed, respectively, to 200 μM ryanodine and daunorubicin through the entire range of test voltages between −90 and 0 mV. The running integrals through both the ON and OFF parts of the responses all increased with time and reached steady values of net charge. A plot of the ON against the OFF charge fell close to the line of equality. The least-squares fits through the origin (lines in both plots) gave slopes of 0.967 ± 0.037 in fibers treated with ryanodine and 0.998 ± 0.057 in fibers exposed to daunorubicin. Neither value deviated significantly from a slope of 1.0 (Student's *t* values of 0.906 and 0.3, with 43° and 37° of freedom for ryanodine- and daunorubicin-treated fibers, respectively.) These findings strongly suggest that the entire charge transfer observed in either daunorubicin or ryanodine is made up of intramembrane capacitative charge.

The present results thus agree with earlier reports that delayed transients were absent in fibers exposed to RyR antagonists and extended such observations to the effects of daunorubicin as well as ryanodine. However, they indicate that conservation persisted through the ON and the OFF parts of imposed voltage steps. This contrasts with the selective fall in ON charge reported by Garcia et al. (1991) that suggested an action of ryanodine mediated solely through its effects on a release of intracellularly stored Ca^{2+} that was in turn responsible for driving delayed charge movement. However, it parallels results from independent kinetic manipulations

through sarcoplasmic reticular Ca^{2+} depletion or loading, which conserved the intramembrane charge (Jong et al., 1995; Pape et al., 1996).

Conservation of Total Charge as a Function of the Holding Potential in Ryanodine and Daunorubicin

The second set of charge conservation tests determined whether ryanodine and daunorubicin altered the maximum charge movement available in the steady state or its variation with holding potential. Fibers were held at a range of membrane potentials altered in 10 mV increments. Each new holding level was maintained for at least 30 s before the sets of test pulse procedures were imposed. Each of these first returned the membrane potential to a −90-mV prepulse level and then imposed a test step to a fixed potential of −20 mV after an interval of 500 ms. This gave test excursions sufficient normally to transfer both q_β and q_γ charge. The experimental records were based on averages of five such sweeps. In turn, every five such test maneuvers were bracketed by sets of +30-mV steps from a −120-mV prepulse level that returned the membrane voltage to −90 mV. Such control runs were made at least 60 s after the holding potential was first returned to fully polarized (−90 mV) values.

Fig. 4 compares results in control fibers (*open squares*), and in preparations exposed to maximally effective ryanodine (*filled circles*) or daunorubicin (*filled triangles*) concentrations. Fig. 4 *A* plots the available steady-state nonlinear charge movement as a function of holding voltage, $Q_{max}(V_H)$, in the absence and in the presence of test agent. Fig. 4, *B* and *C*, show charge movements obtained in response to the fixed test steps through a range of holding potentials each incremented by 10 mV, in fibers exposed to either ryanodine (*B*) or daunorubicin (*C*). All the transients were monotonic decays, as expected from large test excursions to depolarized potentials; these conditions are known to give q_β and q_γ charge species that are both simple decays. The charging currents decreased in amplitude, particularly with the larger shifts in holding potential from −90 mV. Similar values of maximum charge, $Q_{max}(V_H)$, close to 20 nC μF^{-1}, and similar inactivation functions in agreement with those reported on earlier occasions (Huang, 1994*b*), were obtained under all conditions, whether RyR antagonists were present or absent. Thus, the total steady-state charge or the corresponding charge movements were all not affected by small holding potential shifts between −90 and −70 mV, but charge steeply declined with larger changes toward −40 or −50 mV.

The Modified q_γ Isoform Retains Its Steady-state Pharmacological Sensitivity to Tetracaine

Treatment with ryanodine and daunorubicin thus conserved the total steady-state charge Q_{max}, despite the kinetic changes in the q_γ transients. There are two possible explanations for this effect. The q_γ charge species may have undergone a conversion into q_β charge, which is a possibility suggested by Hui and Chandler (1991). This hypothesis would require the entire charge movement to adopt the pharmacological characteristics (including tetracaine resistance) as well as the shallower steady-state voltage dependence ($k \approx 15$–20 mV; Table VII of Hui and Chandler, 1990) expected of the q_β charge. The latter was not borne out in either the charge–voltage ($k \approx 8$–10 mV; Table I) or the inactivation curves ($k \approx 7$–9 mV; Table III), both of which retained their overall steepnesses whether or not antagonist was present. Such findings suggest an alternative scheme that permits q_β and q_γ species to retain their separate steady-state and pharmacological identities despite the kinetic changes.

Fig. 5 displays charge inactivation characteristics in fibers exposed to 2 mM tetracaine. Tetracaine reduced the amplitude of the charge movements and continued to do so after addition of ryanodine (Fig. 5 *A*) or daunorubicin (Fig. 5 *B*). These became monotonic decays of a form and size expected for q_β charge movement. It reduced the available charge, $Q_{max}(V_H)$ as plotted against holding potential, V_H, and reduced the maximum available charge in fully polarized fibers to ~7–9 nC μF^{-1} (Fig. 5 *C*: *open squares*). This situation persisted with the addition of either (200 μM) ryanodine (*filled circles*) or daunorubicin (*filled triangles*). Thus, rather than converting to a tetracaine-resistant form, the charge showed similar declines in $Q_{max}(V_H)$, with holding potential that was characteristic of the q_β system after the q_γ species was blocked by tetracaine. A 50% inactivation under such conditions required a shift in holding level to −20 to −30 mV.

Tetracaine also reduced the steepness of the inactivation functions to expectations for q_β charge in all three cases. Table III displays an analysis of all the inactivation data obtained in both the absence or the presence of tetracaine before and after introduction of RyR antagonists. This complemented the activation data. Thus, in the absence of tetracaine, the steepness factors describing curve fits to single Boltzmann functions were approximately $k \approx 7$–8 mV in the absence of antagonist, and increased only slightly (to 8–9 mV) in ryanodine or daunorubicin. The transition voltages (V^* −47 to −49 mV) were similar under all three conditions. Inclusion of tetracaine uniformly reduced the maximum charge and resulted in shallower inactivation functions ($k \approx 14$–18 mV) characteristic of the potential sensitivity of the q_β as opposed to the q_γ charge.

The q_β Charge in Ryanodine and Daunorubicin

Fig. 6 displays the results of imposing test steps, altered in 10-mV increments, to potentials, V_T, between −90

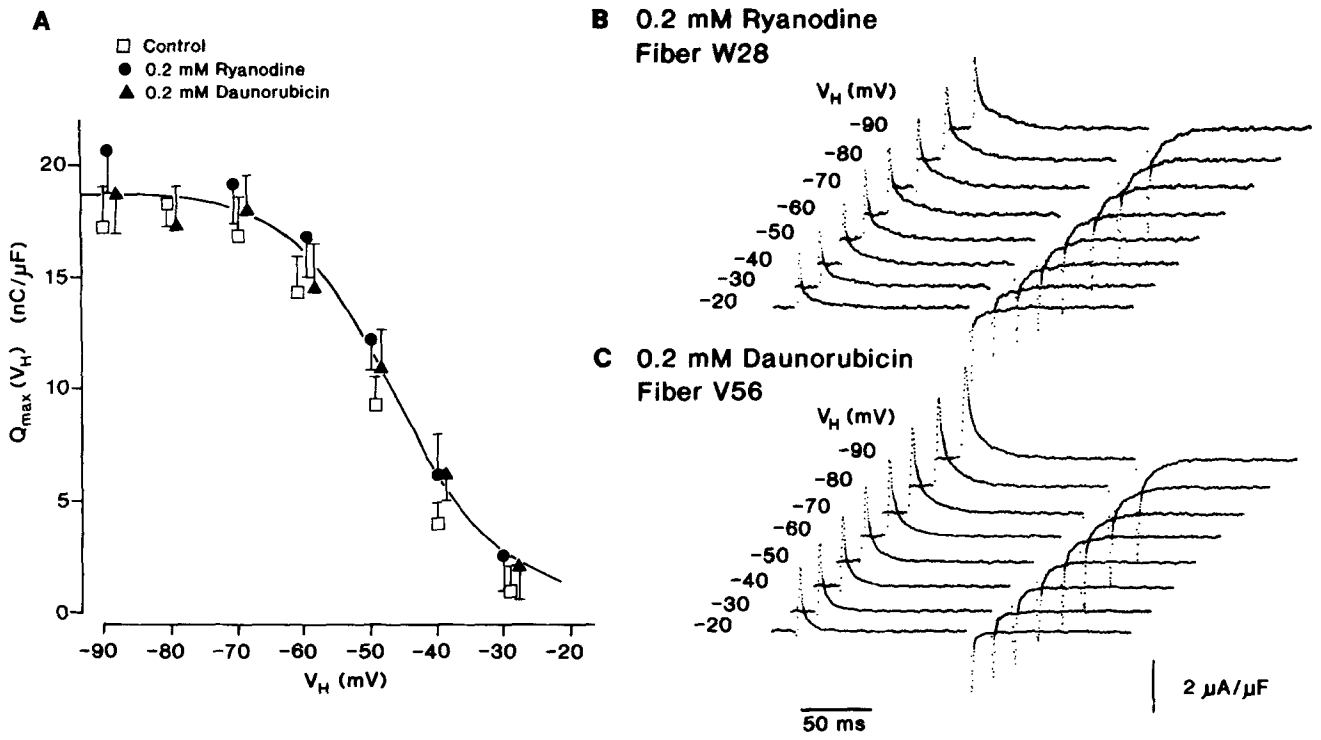

FIGURE 4. Charge inactivation in the presence and absence of ryanodine receptor antagonists. (*A*) Charge displaced by voltage steps between a fixed −90-mV prepulse and a constant −20-mV test voltage and plotted against holding potential V_H in the presence of 200 μM ryanodine (*filled circles*), 200 μM daunorubicin (*filled triangles*), or in control (*open squares*) fibers. (*B, C*) Typical charge movements at the holding potentials obtained in the presence of 200 μM ryanodine (*B*) and 200 μM daunorubicin (*C*). Curves drawn by eye. (*A*) Four control fibers: temperature = 2.7 ± 0.52°C; R_i = 410 ± 7.86 Ω cm. Initial cable constants: λ = 1.7 ± 0.21 mm; r_i = 11,906 ± 1,963 kΩ cm^{-1}; diameter = 70.0 ± 5.2 μm; r_m = 336.7 ± 60.8 kΩ cm; R_m = 6.55 ± 1.12 kΩ cm^2; C_m = 6.6 ± 0.44 μF cm^{-2}. Final cable constants: λ = 1.64 ± 0.22 mm; r_i = 11,570 ± 53.7 kΩ cm^{-1}; diameter = 71.8 ± 7.65 μm; r_m = 267.6 ± 22.9 kΩ cm; R_m = 6.21 ± 1.11 kΩ cm^2; C_m = 7.3 ± 0.44 μF cm^{-2}. Three fibers studied in the presence of 100 μM ryanodine: temperature = 4.1 ± 0.14°C; R_i = 406.8 ± 2.5 Ω cm. Initial cable constants: λ = 1.11 ± 0.02 mm; r_i = 15,587 ± 4,420 kΩ cm^{-1}; diameter = 62.5 ± 7.62 μm; r_m = 196.1 ± 62.8 kΩ cm; R_m = 3.41 ± 0.60 kΩ cm^2; C_m = 10.6 ± 1.8 μF cm^{-2}. Final cable constants: λ = 0.99 ± 0.07 mm; r_i = 16,253 ± 3,172 kΩ cm^{-1}; diameter = 58.9 ± 5.37 μm; r_m = 175.4 ± 59.9 kΩ cm; R_m = 2.95 ± 0.72 kΩ cm^2; C_m = 11.26 ± 1.56 μF cm^{-2}. Five fibers studied in the presence of 200 μM daunorubicin: temperature = 4.6 ± 0.48°C; R_i = 402 ± 6.2 Ω cm. Initial cable constants: λ = 2.1 ± 0.12 mm; r_i = 6,247 ± 782 kΩ cm^{-1}; diameter = 92.5 ± 7.06 μm; r_m = 267.2 ± 12.7 kΩ cm; R_m = 7.7 ± 0.44 kΩ cm^2; C_m = 10.5 ± 0.57 μF cm^{-2}. Final cable constants: λ = 1.9 ± 0.15 mm; r_i = 6,546 ± 1,064 kΩ cm^{-1}; diameter = 91.2 ± 7.8 μm; r_m = 226.7 ± 14.4 kΩ cm; R_m = 6.5 ± 0.59 kΩ cm^2; C_m = 11.1 ± 0.71 μF cm^{-2}. (*B*) Fiber W28 in 200 μM ryanodine: temperature = 4.2°C; R_i = 408.0 Ω cm. Initial cable constants: λ = 1.53 mm; r_i = 7,947 kΩ cm^{-1}; diameter = 80.8 μm; r_m = 186.8 kΩ cm; R_m = 4.74 kΩ cm^2; C_m = 9.2 μF cm^{-2}. Final cable constants: λ = 1.41 mm; r_i = 7,265 kΩ cm^{-1}; diameter = 84.5 μm; r_m = 144.6 kΩ cm; R_m = 3.84 kΩ cm^2; C_m = 10.1 μF cm^{-2}. (*C*) Fiber W56 in 200 μM daunorubicin: temperature = 4.9°C; R_i = 399.0 Ω cm. Initial cable constants: λ = 2.12 mm; r_i = 6,570 kΩ cm^{-1}; diameter = 87.9 μm; r_m = 296.1 kΩ cm; R_m = 8.18 kΩ cm^2; C_m = 11.5 μF cm^{-2}. Final cable constants: λ = 2.07 mm; r_i = 6,042 kΩ cm^{-1}; diameter = 91.6 μm; r_m = 260.8 kΩ cm; R_m = 7.51 kΩ cm^2; C_m = 12.8 μF cm^{-2}.

and 0 mV, in fully polarized muscle fibers exposed to 2 mM tetracaine. Tetracaine again separated a distinct charge component. Nonlinear charge now gradually increased with depolarization (Fig. 6 *C, squares*) to reach a maximum charge reduced to ~10 nC μF^{-1}. Exposure to either ryanodine (Fig. 6, *A* and *C, circles*) or daunorubicin (Fig. 6, *B* and *C, triangles*) preserved this situation. The charge movements remained reduced in amplitude, exponential in form; and gradually increased with depolarization as expected of the q_β species. Table IV demonstrates Boltzmann parameters describing intramembrane charge in 2 mM tetracaine that agreed with independent determinations for q_β charge derived from minimizations to the sum of two Boltzmann functions in both the present (see Table II) and earlier studies (Hui and Chandler, 1990; Hui and Chen, 1992). Neither ryanodine nor daunorubicin altered these values. Thus, all the entries confirm similar reduced values of maximum charge, Q_{max}, and similarly shallow voltage dependences ($k \approx$ 14–16 mV) distinct from those shown by the overall charge in Table I. All these features fulfill expectations for q_β charge in the presence of extracellular gluconate (Chen and Hui, 1991; Huang, 1994*b*).

TABLE III

Analysis of Inactivation Curves $Q_{-20}(V_H)$ from Fibers Studied in the Presence and Absence of 100 or 200 μM Ryanodine or Daunorubicin

Experimental condition	Number of fibers (n)	Maximum charge $Q_{max,-20}$ (nC μF^{-1})	Transition potential V_H* (mV)	Steepness factor k (mV)
0 μM tetracaine				
0 μM ryanodine				
0 μM daunorubicin	4	17.9 ± 0.76	−49.5 ± 0.61	7.6 ± 1.48
0 mM tetracaine				
200 μM ryanodine	3	19.04 ± 0.86	−48.5 ± 1.74	9.0 ± 1.58
0 mM tetracaine				
200 μM daunorubicin	5	18.82 ± 1.09	−47.6 ± 1.94	8.9 ± 1.52
2 mM tetracaine				
0 μM ryanodine				
0 μM daunorubicin	5	7.54 ± 1.32	−34.7 ± 8.56	14.6 ± 4.8
2 mM tetracaine				
200 μM ryanodine	5	6.18 ± 1.01	−31.1 ± 8.03	14.5 ± 3.89
2 mM tetracaine				
200 μM daunorubicin	7	7.72 ± 1.36	−37.6 ± 9.54	17.8 ± 9.14

Least-squares minimizations of maximum charge, $Q_{max,-20}$, transition voltage, V_H*, and slope factor, k (given as means ± SEM), in a single Boltzmann inactivation function given by $Q_{-20}(V_H) = Q_{max,-20}\{1 - 1/\{1 + \exp[-(V_H - V_H^*)/k]\}\}$ for n fibers in each case. Fibers studied in 0 mM or 2 mM tetracaine as indicated.

Steady-state Features of the q_γ Charge

Huang and Peachey (1989) combined data on the overall voltage dependence of intramembrane charge with similar findings on the q_β system in order to derive the steady-state properties of the q_γ charge. Tables V and VI apply a similar approach to investigate the effect of RyR antagonists on the q_γ system. In Table V, data from Fig. 1 *D* were described by the sum of two Boltzmann functions. The values of Q_{max}, V^* and k for the q_γ system were left as free variables, but the corresponding values for the q_β system were obtained from Table IV. This gave q_γ parameters ($Q_{max} \approx 11$ nC μF^{-1}; $V^* \approx -54$ mV, k ≈ 4.2 mV) that agreed with the results of permitting both q_β and q_γ parameters to be free variables (Table II) when RyR antagonists were absent. This independent check for the pharmacological fractionation of intramembrane charge confirmed earlier tests (Hui and Chen, 1992) and further identifies the steeper of the two voltage dependences with a discrete q_γ charge. Ryanodine treatment slightly decreased the q_γ voltage dependence but to a value ($k \approx 5.6$–6.4 mV) nevertheless distinct from that of the q_β system ($k \approx 14.0$–16.0 mV). Conversely, daunorubicin did not significantly alter this voltage dependence ($k \approx 4.0$–5.0 mV).

Table VI summarizes a complementary separation of the inactivation features for q_γ charge. The data in Fig. 4 were similarly approximated to the sum of two Boltzmann inactivation functions for which the q_β parameters were obtained from Table III. The isolated q_β and q_γ inactivation characteristics closely resembled their corresponding activation values. Furthermore, the q_γ steepness factors for inactivation ($k \approx 4.3$–6.6 mV) again were distinct from those of the less voltage-dependent q_β charge ($k \approx 14.0$–18.0 mV). Thus, comparisons of steepness factors for q_β and *isolated* q_γ charge in both charge–voltage (Tables I, IV, and V) and inactivation data (Tables III and VI) strongly emphasize two distinct charge species and confirm that RyR antagonists preserve a separation of their steady-state and pharmacological identities despite the kinetic changes.

Finally, Fig. 7 summarizes the overall steady-state properties as generated by the analyses in Tables I to VI. The symbols in Fig. 7 *A* reconstitute the charge–voltage curves that arise from the distinct q_β and q_γ charge contributions, as separated by the least squares minimizations either to the sum of two Boltzmann functions (Table II, *open squares*) or by the empirical pharmacological approach (Tables IV and V, *filled squares*). The resulting functions were closely concordant. Both steeply increased with depolarization beyond −60 mV, then more gradually tended to a maximum charge of around 20 nC μF^{-1} with large test steps. The resulting model that incorporated such distinct q_β and q_γ charge contributions with distinct steepness factors also successfully predicted the charge–voltage curves that would result from introduction of either ryanodine (*circles*) or daunorubicin (*triangles*) at 100-μM (*open symbols*) or 200-μM concentrations (*filled symbols*), while permitting a consistent ~10-mV shift in transition potential for the q_γ charge (cf. Table V). The model also reproduced the corresponding q_β charge–voltage curves derived from tetracaine-treated fibers

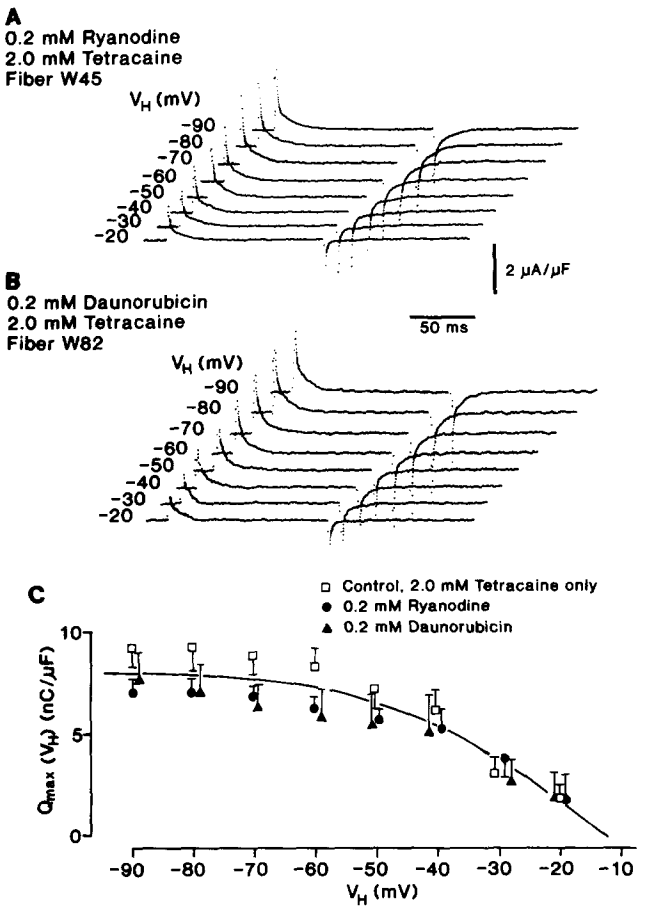

FIGURE 5. Inactivation characteristics after charge fractionation by 2 mM tetracaine. (*A*, *B*) Typical charge movements from fibers exposed to 2 mM tetracaine at different holding potentials V_H obtained in the presence of 200 μM ryanodine (*A*) and 200 μM daunorubicin (*B*). (*C*) Charge movement in response to voltage steps between a fixed −90-mV prepulse and a constant −20-mV test voltage plotted against holding potential V_H in the presence of 200 μM ryanodine (*filled circles*), 200 μM daunorubicin (*filled triangles*), or in control fibers (*open squares*) in tetracaine containing solutions. Curve drawn by eye. (*A*) Fiber W45 studied in the presence of 200 μM ryanodine: temperature = 3.9°C; R_i = 412 Ω cm; λ = 1.45 mm; r_i = 11,114.7 kΩ cm^{-1}; diameter = 68.7 μm; r_m = 232.2 kΩ cm; R_m = 5.01 kΩ cm^2; C_m = 9.3 μF cm^{-2}. Final cable constants: λ = 1.18 mm; r_i = 10,317 kΩ cm^{-1}; diameter = 71.3 μm; r_m = 144.4 kΩ cm; R_m = 3.23 kΩ cm^2; C_m = 11.9 μF cm^{-2}. (*B*) Fiber W84 studied in the presence of 200 μM daunorubicin: temperature = 2.4°C; R_i = 390.2 Ω cm. Initial cable constants: λ = 1.76 mm; r_i = 9,241 kΩ cm^{-1}; diameter = 73.3 μm; r_m = 285.1 kΩ cm; R_m = 6.57 kΩ cm^2; C_m = 9.2 μF cm^{-2}. Final cable constants: λ = 1.93 mm; r_i = 6,826 kΩ cm^{-1}; diameter = 85.3 μm; r_m = 254 kΩ cm; R_m = 6.80 kΩ cm^2; C_m = 10.8 μF cm^{-2}. (*C*) Five fibers studied in the absence of test agent: temperature = 5.5 ± 0.1°C; R_i = 366.1 ± 1.1 Ω cm. Initial cable constants: λ = 1.7 ± 0.20 mm; r_i = 8,736 ± 2,494 kΩ cm^{-1}; diameter = 80.0 ± 10.7 μm; r_m = 238 ± 57.7 kΩ cm; R_m = 5.57 ± 0.92 kΩ cm^2; C_m = 5.53 ± 0.64 μF cm^{-2}. Final cable constants: λ = 1.49 ± 0.17 mm; r_i = 9,330 ± 2,901 kΩ cm^{-1}; diameter = 78.2 ± 10.8 μm; r_m = 187 ± 37.7 kΩ cm; R_m = 4.3 ± 0.56 kΩ cm^2; C_m = 6.6 ± 0.99 μF cm^{-2}. Five fibers studied in the presence of 200 μM ryanodine: temperature = 4.6 ± 0.37°C; R_i = 403.2 ± 4.72 Ω cm; λ = 1.49 ± 0.06 mm; r_i = 7,336 ± 1,210 kΩ cm^{-1}; diameter = 86.7 ± 6.73 μm; r_m = 159.9 ± 22.5 kΩ cm; R_m = 4.19 ± 0.33 kΩ cm^2; C_m = 12.8 ± 1.11 μF cm^{-2}. Final cable constants: λ = 1.27 ± 0.07 mm; r_i = 6,841 ± 1,169 kΩ cm^{-1}; diameter = 90.52 ± 8.31 μm; r_m = 109.03 ± 14.33 kΩ cm; R_m = 2.98 ± 0.23 kΩ cm^2; C_m = 14.05 ± 0.88 μF cm^{-2}. Seven fibers studied in the presence of 200 μM daunorubicin: temperature = 2.9 ± 0.16°C; R_i = 384 ± 1.9 Ω cm. Initial cable constants: λ = 3.3 ± 0.67 mm; r_i = 5,661 ± 1,380 kΩ cm^{-1}; diameter = 116.7 ± 17.86 μm; r_m = 352.8 ± 43.7 kΩ cm; R_m = 14.23 ± 3.68 kΩ cm^2; C_m = 12.4 ± 1.73 μF cm^{-2}. Final cable constants: λ = 2.53 ± 0.45 mm; r_i = 5,560 ± 1,477 kΩ cm^{-1}; diameter = 125.2 ± 8.44 μm; r_m = 245.1 ± 36.1 kΩ cm; R_m = 8.90 ± 2.10 kΩ cm^2; C_m = 12.66 ± 1.49 μF cm^{-2}.

(*squares*) and correctly predicted that these did not significantly vary after ryanodine (*circles*) or daunorubicin treatment (*triangles*). This confirmed expectations from a situation in which the RyR antagonists did not influence q_β charge (Fig. 7 *B*). Finally, the model of additive q_β (Table III) and q_γ charge contributions (Table VI) also accommodated the charge inactivation findings both before (Fig. 7 *C*, *upper plot*) and after (Fig. 7 *C*, *lower plot*) q_γ charge was abolished by tetracaine treatment, whether ryanodine (*circles*) or daunorubicin (*triangles*) was present or absent (*squares*).

DISCUSSION

Skeletal muscle charge movements include contributions from both tetracaine-resistant q_β and tetracaine-sensitive q_γ species. The steeply voltage-dependent q_γ component contributes delayed ("hump") currents in response to threshold depolarizations in both amphibian (Adrian and Peres, 1979; Huang, 1981*a*; Hui, 1983; Hui and Chandler, 1990; Vergara and Caputo, 1982) and mammalian skeletal muscle (Simon and Beam, 1985; Lamb, 1986; Hollingworth et al., 1990), in contrast to the rapid monotonic decays and shallow voltage dependence shown by q_β charge. Charge movements may be instrumental in the control of sarcoplasmic reticular Ca^{2+} release by the transverse tubular potential during excitation–contraction coupling (Schneider and Chandler, 1973). Complex (q_γ) charging waveforms appear specifically to occur in skeletal muscle in which excitation–contraction coupling may involve direct allosteric interactions between DHPR-voltage sensors and RyR-Ca^{2+} release channels (for review see Huang, 1993). In contrast, the Ca^{2+} channel gating currents that also initiate elevations of cytosolic Ca^{2+} in arthropod skeletal muscle and mammalian cardiac muscle are simple monotonic decays whose associated charge nevertheless also exhibits steep steady-state voltage dependences similar to those of the q_γ system (Gilly and Scheuer, 1984; Bean and Rios, 1989). However,

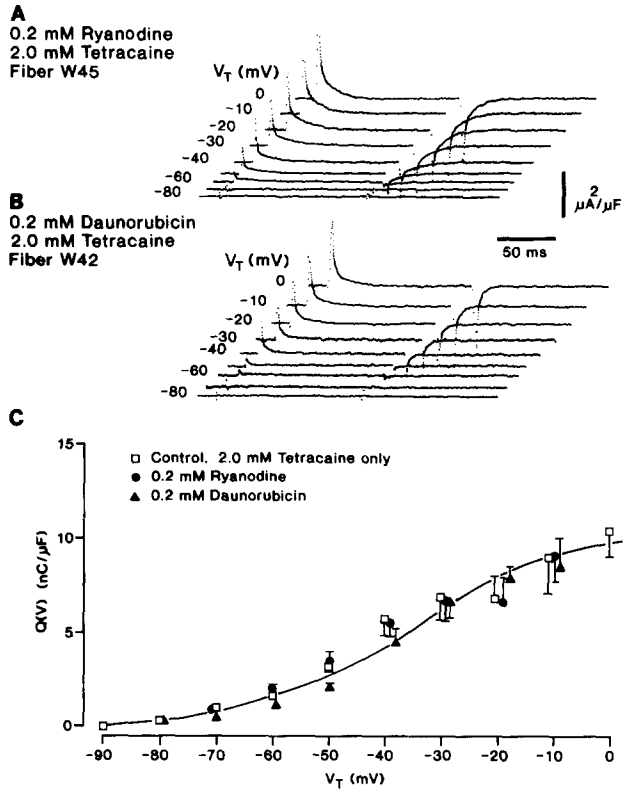

FIGURE 6. Charge movements after exposure to 2 mM tetracaine. (*A*, *B*) Typical charge movements at fully polarized (−90 mV) holding potentials obtained in the presence of 200 μM ryanodine (*A*) and 200 μM daunorubicin (*B*) after test steps of graded size. (*C*) Charge–voltage curves in response to test voltage steps of different amplitude taken from the −90-mV holding potential plotted against the potential V_T in presence of 200 μM ryanodine (*filled circles*), 200 μM daunorubicin (*filled triangles*), or in control (*open squares*) fibers in tetracaine containing solutions. Curve drawn by eye. (*A*) Fiber W45 studied in the presence of 200 μM ryanodine: temperature = 3.9°C; R_i = 412 Ω cm; λ = 1.45 mm; r_i = 11,114.7 kΩ cm^{-1}; diameter = 68.7 μm; r_m = 232.2 kΩ cm; R_m = 5.01 kΩ cm^2; C_m = 9.3 μF cm^{-2}. Final cable constants: λ = 1.18 mm; r_i = 10,317 kΩ cm^{-1}; diameter = 71.3 μm; r_m = 144.4 kΩ cm; R_m = 3.23 kΩ cm^2; C_m = 11.9 μF cm^{-2}. (*B*) Fiber W42 studied in the presence of daunorubicin: temperature = 4.8°C; R_i = 400.0 Ω cm; λ = 2.04 mm; r_i = 7,926 kΩ cm^{-1}; diameter = 80.2 μm; r_m = 328.2 kΩ cm; R_m = 8.26 kΩ cm^2; C_m = 11.9 μF cm^{-2}. Final cable constants: λ = 1.34 mm; r_i = 8,717 kΩ cm^{-1}; diameter = 76.4 μm; r_m = 156.4 kΩ cm; R_m = 3.75 kΩ cm^2; C_m = 13.3 μF cm^{-2}. (*C*) Six fibers studied in the absence of test agent. Initial cable constants: temperature = 5.4 ± 0.1°C; R_i = 367.6 ± 1.16 Ω cm; λ = 2.39 ± 0.235 mm; r_i = 6,899 ± 1,566 kΩ cm^{-1}; diameter = 93.8 ± 12.3 μm; r_m = 334.7 ± 46.8 kΩ cm; R_m = 9.14 ± 0.79 kΩ cm^2; C_m = 7.13 ± 1.3 μF cm^{-2}. Final cable constants: λ = 2.1 ± 0.25 mm; r_i = 7,691 ± 1,746 kΩ cm^{-1}; diameter = 90.0 ± 13.03 μm; r_m = 268.7 ± 40.2 kΩ cm; R_m = 6.88 ± 0.45 kΩ cm^2; C_m = 7.94 ± 1.67 μF cm^{-2}. Ten fibers studied in the presence of 200 μM ryanodine: temperature = 4.51 ± 0.16°C; R_i = 407.3 ± 4.04 Ω cm; λ = 2.09 ± 0.21 mm; r_i = 7,424 ± 1,045 kΩ cm^{-1}; diameter = 92.6 ± 7.09 μm; r_m = 265 ± 25.1 kΩ cm; R_m = 7.74 ± 1.12 kΩ cm^2; C_m = 10.6 ± 0.6 μF cm^{-2}. Final cable constants: λ = 2.04 ± 0.32 mm; r_i = 6,112 ± 933 kΩ cm^{-1}; diameter = 100.8 ± 8.51 μm; r_m = 216.8 ± 38.6 kΩ cm; R_m = 7.17 ± 1.91 kΩ cm^2; C_m = 12.4 ± 0.67 μF cm^{-2}. Eight fibers studied in the presence of daunorubicin: temperature = 3.7 ± 0.22°C; R_i = 411 ± 2.8 Ω cm. Initial cable constants: λ = 1.8 ± 0.11 mm; r_i = 7,948 ± 1,024 kΩ cm^{-1}; diameter = 84.4 ± 4.4 μm; r_m = 252.7 ± 39.3 kΩ cm; R_m = 6.5 ± 0.75 kΩ cm^2; C_m = 9.99 ± 0.70 μF cm^{-2}. Final cable constants: λ = 1.49 ± 0.91 mm; r_i = 7,689 ± 1,063 kΩ cm^{-1}; diameter = 86.8 ± 5.35 μm; r_m = 175.4 ± 31.1 kΩ cm; R_m = 4.48 ± 0.62 kΩ cm^2; C_m = 10.6 ± 0.96 μF cm^{-2}.

these latter systems may be indirectly activated by a triggering entry of extracellular Ca^2 rather than through such direct receptor–receptor couplings (Beuckelman and Wier, 1988; Fabiato, 1985; Sun et al., 1995). The question then arises whether the complex q_γ kinetics in skeletal muscle specifically reflect allosteric interactions between the molecules that initiate excitation–contraction coupling.

The present study explored whether RyR modification might influence the properties of intramembrane charge through such mechanical couplings. Thus, a hypothesis that RyR gating is allosterically coupled to configurational changes in dihydropyridine receptors (DHPRs) would predict that such interactions are reciprocal and that RyR modification in turn should influence intramembrane charge. The use of ryanodine was prompted by earlier reports in cut fibers (Garcia et al., 1991). The present experiments also used daunorubicin as a test agent for the first time and examined not only charge activation but inactivation and conservation properties. They further assessed the extent to which q_γ and q_β charge species retained their separate identity after antagonist treatment. Ryanodine (0.1–500 μM) specifically inactivates Ca^{2+} release in isolated rabbit junctional SR membranes, given optimum equilibrium conditions for receptor binding (Zimanyi et al., 1992; Rouseau et al., 1987; Meissner, 1994). Anthraquinones such as daunorubicin are cardiotoxic cancer chemotherapeutic agents (Dodd et al., 1993) that act on sarcoplasmic reticular Ca^{2+} release channels in lipid bilayers (Holmberg and Williams, 1990) and specifically influence ryanodine binding to sarcoplasmic reticular membranes and soluble receptor preparations (Pessah et al., 1990; Bowling et al., 1994). They alter Ca^{2+} movements and tension generation in guinea-pig cardiac muscle at concentrations (100–200 μM) similar to those used here (Hagane et al., 1988).

Cooled, intact amphibian muscle fibers were studied in experimental configurations that permitted regular determinations of linear fiber cable constants (cf. Huang, 1994*a*). None of the explored test agents significantly influenced linear capacitance in fibers of comparable diameter, in contrast to the 20–40% reduction reported in tetracaine-treated fibers studied in a Vase-

TABLE IV

Analysis of Charge Voltage Curves Q(V) from Fibers Studied in the Presence and Absence of 100 or 200 μM Ryanodine or Daunorubicin

Fiber condition (μM ryanodine; μM daunorubicin)	Number of fibers (n)	Maximum charge Q_{max} (nC μF^{-1})	Transition potential V^* (mV)	Steepness factor k (mV)
Control:				
0 μM ryanodine				
0 μM daunorubicin	6	9.2 ± 2.67	−37.1 ± 11.12	14.1 ± 7.25
2 mM tetracaine				
200 μM ryanodine	10	10.7 ± 1.62	−37.5 ± 6.93	15.3 ± 1.56
2 mM tetracaine				
200 μM daunorubicin	8	13.83 ± 2.9	−25.3 ± 8.97	15.7 ± 4.43

Fibers studied in 2 mM tetracaine to isolate q_β charge. Least-squares minimizations to determine maximum charge, Q_{max}, transition voltage, V^*, and slope factor, k (given as means ± SEM), in a single Boltzmann function given by $Q(V) = Q_{max}/\{1 + \exp[-(V - V^*)/k]\}$ for n fibers in each case.

line gap (Garcia et al., 1991). Prominent, delayed q_γ currents followed the early q_β decays at threshold potentials close to contractile threshold in cooled fibers exposed to gluconate-containing hypertonic solutions in the absence of test reagents. Other cut-fiber preparations have shown only a simple monotonic decay attributed to a single (q_β) component with a shallow voltage dependence (steepness factor, $k \approx$ 13–21 mV; Hui and Chandler, 1990, Table VII). Nevertheless, the present findings confirm reports in both intact (Adrian and Peres, 1979; Huang and Peachey, 1989; Hui, 1983) and other cut-fiber (Hui and Chandler, 1990, 1991) preparations that monitored fiber cable properties, whether their pulse procedures used small (e.g., Adrian and Peres, 1979; Huang, 1982; Huang and Peachey, 1989) or large voltage steps. These latter studies all related the delayed charging transients to a steeply varying contribution to steady-state charge voltage curves and so specifically identified q_β and q_γ with distinguishable steady-state components of the nonlinear charge localized in different regions of muscle membrane (Huang and Peachey, 1989; Hui and Chandler, 1990).

Ryanodine and daunorubicin converted the normally complex q_γ waveforms to simple exponential decays that thus became cotemporal with and indistinguishable from the q_β relaxations, indicative of the parallel transitions, independent of q_β charge, suggested previously (Huang, 1994*b*). The corresponding charge–voltage relationships showed positive (~10 mV) local shifts over the membrane potentials through which the delayed currents would have taken place. Garcia et al. (1991) similarly reported that ryanodine (1–100 μM) abolished delayed charge movement but described a 5.0 nC μF^{-1} reduction in ON charge movement but

TABLE V

Isolation of the Boltzmann Parameters of Maximum Charge, Q_{max}, Transition Voltage, V^*, and Slope Factor k (Given as Means ± SEM), for the q_γ Charge

Fiber condition (μM ryanodine; μM daunorubicin)	Number of fibers (n)	Maximum charge Q_{max} (nC μF^{-1})	Transition potential V^* (mV)	Steepness factor k (mV)
Control:				
0 μM ryanodine				
0 μM daunorubicin	7	11.3 ± 0.4	−53.5 ± 1.47	4.2 ± 1.08
100 μM ryanodine				
0 μM daunorubicin	4	10.14 ± 0.68	−40.9 ± 1.24	5.7 ± 1.22
200 μM ryanodine				
0 μM daunorubicin	5	9.63 ± 0.39	−42.4 ± 1.66	6.4 ± 1.03
0 μM ryanodine				
100 μM daunorubicin	6	8.1 ± 0.56	−41.8 ± 2.15	4.04 ± 1.76
0 μM ryanodine				
200 μM daunorubicin	4	11.7 ± 0.16	−43.0 ± 1.94	5.01 ± 1.11

Charge voltage curves $Q(V)$ from fibers studied in tetracaine-free solutions before and after addition of 100 or 200 μM of either ryanodine or daunorubicin. Least-squares minimizations were made to the sum of two Boltzmann terms $\Sigma Q(V) = Q_\beta(V) + Q_\gamma(V)$ each given by an equation of the form $Q(V) = Q_{max}/\{1 + \exp[-(V - V^*)/k]\}$ with the parameters for the $Q_\beta(V)$ term obtained from Table IV.

TABLE VI

Isolation of Values of Maximum Charge, Q_{max}, Transition Voltage, V_H, and Slope Factor, k, for q_γ Charge Inactivation as Described by a Single Boltzmann Function*

Fiber condition (μM ryanodine; or μM daunorubicin)	Number of fibers (n)	Maximum charge Q_{max} (nC μF^{-1})	Transition potential V_H^* (mV)	Steepness factor k (mV)
Control:				
0 μM ryanodine				
0 μM daunorubicin	4	10.4 ± 0.64	−54.6 ± 1.98	4.3 ± 1.51
100 μM ryanodine				
0 μM daunorubicin	3	12.63 ± 0.74	−52.5 ± 1.94	6.6 ± 1.73
200 μM ryanodine				
0 μM daunorubicin	5	11.01 ± 0.94	−53.0 ± 2.27	5.8 ± 1.79

Inactivation curves from fibers studied in tetracaine-free solutions before and after addition of 200 μM of ryanodine or daunorubicin. Least-squares minimizations of inactivation data, $Q_{max}(V_H)$, were made to the sum of two Boltzmann terms $\Sigma Q(V_H) = Q_\beta(V_H) + Q_\gamma(V_H)$ where each term is described by an inactivation equation of the form $Q_{-20}(V_H) = Q_{max,-20}\{1 - 1/[1 + \exp[-(V_H - V_H^*)/k]]\}$ with the values for the Q_β (V) term obtained from Table III.

not in the steady-state OFF charge and a resulting disruption of charge conservation. The latter observations reinforced a scheme that required only a single (q_β) intramembrane charge species that had a relatively shallow voltage dependence ($k \approx$ 11–15 mV; Pizarro et al., 1991). This could trigger an initial release of intracellularly stored Ca^{2+} into the space between transverse tubules and sarcoplasmic membrane. It was suggested that a resulting Ca^{2+} binding to tubular membrane would alter its surface potential and so drive additional delayed (q_β) charge movement, defined kinetically as a q_γ current. Ryanodine would influence such Ca^{2+} release. Such schemes were prompted by the observations of late inward-going phases that followed "humps" isolated from ON charge movement waveforms, as these could reflect the subsequent diffusion of Ca^{2+} away from that space. There were also the complexities observed in the biphasic OFF charge movements and their smaller integrals compared with the ON transients (Csernoch et al., 1991; Pizarro et al., 1991; Szucs et al., 1991; see also Hui, 1994).

However, the experimental conditions adopted here resulted in complete decays to steady DC levels without intervening inward-going phases or other time-dependent currents. Furthermore, the net ON and OFF charge transfers stayed equal. Finally, approximation of a single two-state Boltzmann analysis to the charge–voltage curves suggested that RyR antagonists preserved the total charge Q_{max} despite the kinetic changes. The findings thus parallel results from independent manipulations that altered q_γ kinetics but preserved the distinct q_β and q_γ transitions with their different properties, their total quantity, and their ON–OFF conservation, when sarcoplasmic reticular Ca^{2+} content was depleted (to <10 μM) or increased (Jong et al., 1995; Pape et al., 1996; but see also Polakova and Heiny, 1994). Such findings were compatible with an intramembrane q_γ charge primarily driven by tubular voltage change (Huang and Peachey, 1989; Huang, 1993, 1994*a*, 1994*b*; Hui and Chandler 1990).

A closer scrutiny of charge–voltage data threw light on the mechanism by which RyR antagonists might influence intramembrane charge. On the one hand, the q_γ charge could interconvert into the q_β species. The entire charge then would acquire not only its kinetic properties but also its more gradual steady-state voltage dependence and the tetracaine resistance of q_β charge. Hui and Chandler (1990, 1991) suggested that q_γ currents could reflect cooperative rearrangements of groups of interacting DHPRs, whereas q_β currents could result from independent rearrangements of individual but otherwise identical receptors. Alternatively, RyR antagonists could transform q_γ charge into an exponentially relaxing isoform that otherwise retained steady-state and pharmacological properties distinct from those of q_β charge. Ryanodine, but not daunorubicin slightly altered the steepness of the overall charge–voltage curves, but these ($k \approx$ 7–9 mV) nevertheless remained compatible with persistent q_γ contributions as opposed to a transformation into the gradually varying q_β charge ($k \approx$ 15–19 mV). Additionally, RyR modification also preserved the maximum charge in, and the steepness ($k \approx$ 7–9 mV) of, inactivation curves. Jong et al. (1995) and Pape et al. (1996) similarly reported persistently steep charge–voltage relationships ($k \approx$ 7 mV) characteristic of a q_γ contribution, whether fibers were depleted of, or loaded with, Ca^{2+}.

These possibilities were further explored in experiments that specifically separated q_γ and q_β changes from the charge–voltage and inactivation curves through their electrical and pharmacological properties. Tetracaine influences Ca^{2+} channel function in rat neurones (Sugiyama and Muteki, 1994), and in frog and arthropod muscle (Garcia et al., 1991; Scheuer and Gilly,

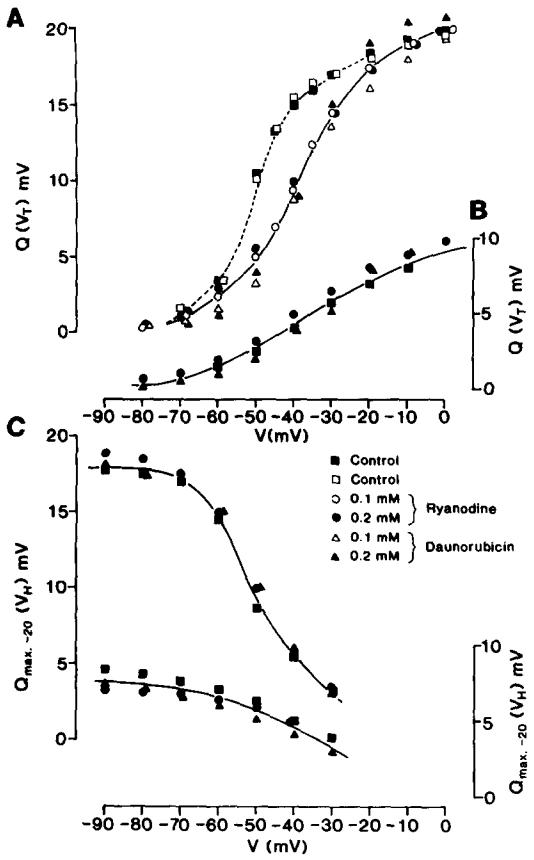

FIGURE 7. Summary of overall steady-state charge movement properties predicted from the incorporation of discrete q_β and q_γ contributions to intramembrane charge. Data points represent charge–voltage functions derived from each individual analysis in Tables I to VI. Curves drawn by eye. (*A*; *left ordinate*) Charge–voltage curves constituted from distinct q_β and q_γ charge contributions as determined by least-squares minimizations of empirical data either to the sum of two Boltzmann functions (*open squares*) or by an empirical pharmacological approach before introduction of RyR antagonists (*filled squares*). These provide controls for the predicted functions that result from the introduction of either ryanodine (*circles*) or daunorubicin (*triangles*) at 100 (*open symbols*) or 200 μM concentrations (*filled symbols*). (*B*; *right ordinate*) The corresponding q_β charge–voltage curves from fibers exposed to tetracaine before (*filled squares*) or after ryanodine (*filled circles*) or daunorubicin treatment (*filled triangles*). (*C*) Reconstruction of charge inactivation findings before (*upper plot*; *left ordinate*) and after the q_γ contribution was abolished by tetracaine treatment (*lower plot*; *right ordinate*) in the absence (*filled squares*) or presence of ryanodine (*filled circles*) or daunorubicin (*filled triangles*) after a similar use of additive q_β and q_γ contributions.

1986), besides the q_γ charge movements linked to DHPR function in skeletal muscle (Huang, 1990). Nevertheless, it provides a consistent empirical charge separation testable against a wide range of independent criteria. Thus, a rigorous comparison of results from (*1*) defining tetracaine-sensitive charge as q_γ and tetracaine resistant charge as q_β (Huang, 1982); against (*2*) mathematical techniques based on the original kinetic definitions of q_β and q_γ in "on" transients (Hui, 1983); (*3*) fitting charge–voltage functions to the sum of two independent Boltzmann distributions (Hui and Chandler, 1990); and (*4*) kinetic q_γ isolations after partial repolarizations to around −60 mV (see Hui and Chandler, 1991), all yielded quantitatively consistent charge separations (Hui and Chen, 1992, Table III). They further confirmed that any changes in q_β charge were too small to post any action of tetracaine on other than q_γ charge. Hui and Chen (1992) also established that tetracaine concentrations of >0.5–1.0 mM were required to accomplish such full separations. Scrutinies of both fiber stability and cable constants confirm that use of 2 mM tetracaine permitted viable and stable intact fiber preparations in the present experiments. Lower concentrations (0.1–0.5 mM) only partially suppressed q_γ charge, while still shifting the charge–voltage curves; micromolar levels (≈25 μM; cf. Csernoch et al., 1991) only altered q_γ kinetics (Hui and Chen, 1992).

This separation excluded the possibility that the application of RyR antagonists brought about a conversion of q_γ to (tetracaine-resistant) q_β charge. Thus, treatment with tetracaine consistently and similarly reduced the total charge Q_{max}, whether such antagonists were present or absent. The charge movements became reduced in size and exponential decays. Thus, RyR antagonists do not convert charge from a tetracaine-sensitive to a tetracaine-resistant q_β form. Both the charge–voltage and the inactivation curves also exhibited reduced voltage dependences ($k \approx$ 14–18 mV) that were distinct from those of either total ($k \approx$ 7–9 mV) or of isolated q_γ charge and that were characteristic of q_β charge movement. These changes were observed whether or not RyR antagonists were present or absent. It therefore continued to be possible to separate q_β and q_γ contributions to charge–voltage curves in the presence of RyR antagonists. This characterization made it possible to isolate the features of the q_γ contributions to charge–voltage curves.

Such an isolation was first applied to charge–voltage curves from untreated fibers in terms of the sum of two Boltzmann functions. The results from leaving both q_β and q_γ contributions as free variables (Hui and Chandler, 1990) (see Table II) confirmed a second approach that assumed experimentally determined parameters for q_β charge from tetracaine-treated fibers (cf. Huang and Peachey, 1989; Hui and Chen, 1992). Thus both procedures confirmed clearly different slope factors for q_γ ($k \approx$ 4–6 mV) and q_β ($k \approx$ 14–16 mV) charge. Such an analysis further yielded similar steepness factors for q_γ charge ($k \approx$ 4–6 mV) that further emphasized their differences from those of q_β charge ($k \approx$ 14–16 mV) in both control fibers and in fi-

bers exposed to ryanodine or daunorubicin. A corroborating, independent analysis of the inactivation characteristics of q_γ charge also yielded sharply contrasting steepness factors for q_β ($k \approx 14$–17 mV) and q_γ charge ($k \approx 4$–6 mV). Thus, q_β and q_γ charge species retained their distinct steady-state charge–voltage and inactivation identities even after the kinetic modifications of the q_γ charge species brought about by RyR antagonists.

Charge movements signal dielectric events within voltage-clamped transverse tubular membranes. Electrical (Rios and Brum, 1987; Huang, 1990) and genetic (Takekura et al., 1994, 1995) studies implicate intramembrane DHPRs as the voltage sensors that initiate excitation–contraction coupling. Yet, the present studies demonstrate that RyR modifications alter the kinetics particularly of q_γ transients, even though the RyR resides in membranes of the terminal cisternae, from which the tubules are electrically isolated (see review in Huang, 1993). Recent depletions or loadings of sarcoplasmic reticular Ca^{2+} have similarly accomplished kinetic changes while preserving the steady-state characteristics and individual identities of the component charge species (Jong et al., 1995; Pape et al., 1996). These suggest that altered conditions of intracellular Ca^{2+} resulting from Ca^{2+} release channel modification might cause such changes.

The present results, taken with the observed associations of four DHPRs with each RyR in skeletal muscle triads (see reviews in Meissner, 1994; Franzini-Armstrong and Jorgenson, 1994) suggest an alternative or coexistent mechanism. Recent biochemical evidence (Anderson and Meissner, 1995) suggests that DHPRs are linked allosterically to RyR-I or the RyR-α isoforms in mammalian or amphibian skeletal muscle triads, respectively (Olivares et al., 1991), but not to the RyR-II isoforms in cardiac muscle (Sun et al., 1995). Such a scheme would still permit DHPRs to generate a steady-state q_γ charge transfer driven by transverse tubular potential (cf. Huang, 1994*a*, 1994*b*) that is sensitive to inhibition by the calcium channel reagents tetracaine (see above) and to voltage-dependent block by nifedipine (Huang, 1982, 1990). However, the kinetic complexities shown by q_γ charge movements might then reflect reciprocal allosteric interactions (Huang, 1983, 1984) between RyR-Ca^{2+} release channels and DHPR-voltage sensors. RyR modification then could convert the complex q_γ charge movement into an alternative quasi-exponential kinetic isoform while leaving the distinct steady-state and pharmacological features of both q_γ and q_β charge intact. Such schemes relating q_γ "humps" to proposed direct allosteric interactions between DHPRs and RyRs in skeletal muscle may merit further investigation and testing.

The author thanks B. Secker, W. Smith, and M. Swann for skilled assistance, the Royal Society for partial equipment support, and Prof. W.K. Chandler for helpful discussions and preprints of his work.

Original version received 26 June 1995 and accepted version received 4 January 1996.

REFERENCES

Adrian, R.H., W.K. Chandler, and A.L. Hodgkin. 1969. The kinetics of mechanical activation in frog muscle. *J. Physiol.* 204:207–230.

Adrian, R.H., and A. Peres. 1979. Charge movement and membrane capacity in skeletal muscle. *J. Physiol.* 289:83–97.

Anderson, K., and G. Meissner. 1995. T tubule depolarization-induced SR Ca^{2+} release is controlled by dihydropyridine receptor- and Ca^{+}-dependent mechanisms in cell homogenates from rabbit skeletal muscle. *J. Gen. Physiol.* 105:363–383.

Baylor, S.M., S. Hollingworth, and M.W. Marshall. 1989. Effects of intracellular ruthenium red on excitation-contraction coupling in intact frog skeletal muscle fibres. *J. Physiol.* 408:617–635.

Bean, B.P., and E. Rios. 1989. Non-linear charge movement in the membranes of mammalian cardiac muscle cells. Components from Na and Ca channel gating. *J. Gen. Physiol.* 94:65–93.

Beuckelmann, D.J., and W.G. Wier. 1988. Mechanism of release of calcium from sarcoplasmic reticulum of guinea-pig cardiac cells. *J. Physiol.* 405:233–255.

Bowling, N., D.E. Mais, K. Getzon, and A.M. Watanabe. 1994. Ryanodine and an iodinated analog: doxorubicin effects on binding and Ca^{2+} accumulation in cardiac sarcoplasmic reticulum. *Euro. J. Pharmacol.* 268:365–373.

Cannell, M.B., H. Cheng, and W.J. Lederer. 1995. The control of calcium release in heart muscle. *Science (Wash. DC).* 268:1045–1049.

Chandler, W.K., and C.S. Hui. 1990. Membrane capacitance in frog cut twitch fibers mounted in a double vaseline-gap chamber. *J. Gen. Physiol.* 96:225–256.

Chen, W., and C.S. Hui. 1991. Gluconate suppresses Q_γ more effectively than Q_β in frog twitch fibers. *Biophys. J.* 59:543*a* (Abstr.)

Csernoch, L., G. Pizarro, I. Uribe, M. Rodriguez, and E. Rios. 1991. Interfering with calcium release supresses I_γ, the hump component of intramembranous charge movement in skeletal muscle. *J. Gen. Physiol.* 97:845–884

Dodd, D.A., J.B. Atkinson, R.D. Olson, S. Buck, B.J. Cusack, S. Fleischer, and R.J. Boucek, Jr. 1993. Doxorubicin cardiomyopathy is associated with a decrease in calcium release channel of the sarcoplasmic reticulum in a chronic rabbit model. *J. Clin. Invest.* 91: 1697–1705.

Fabiato, A. 1985. Time and calcium dependence of activation and inactivation of calcium-induced release of calcium from the sarcoplasmic reticulum of a skinned canine cardiac Purkinje cell. *J. Gen. Physiol.* 85:247–289.

Franzini-Armstrong, C., and A.O. Jorgensen. 1994. Structure and development of E-C coupling units in skeletal muscle. *Annu. Rev. Physiol.* 56:509–534.

Fryer, M.W., G.D. Lamb, and I.R. Neering. 1989. The action of ryanodine on rat fast and slow intact skeletal muscle fibers. *J. Physiol.* 414, 399–413.

Garcia, J., A.J. Avila-Sakar, and E. Stefani. 1991. Differential effects of ryanodine and tetracaine on charge movement and calcium transients in frog skeletal muscle. *J. Physiol.* 440:403–417.

Gilly, W.F., and T. Scheuer. 1984. Contractile activation in scorpion striated muscle fibers. Dependence on voltage and external calcium. *J. Gen. Physiol.* 84:321–345.

Hagane, K., T. Akera, and J.R. Berlin. 1988. Doxorubicin: mechanism of cardiodepressant actions in guinea pigs. *J. Pharmacol. Exp. Ther.* 246:655–661.

Hodgkin, A.L., and S. Nakajima. 1972. The effects of diameter on the electrical constants of frog skeletal muscle fibers. *J. Physiol.* 221:105–120.

Hollingworth, S., M.W. Marshall, and E. Robson. 1990. The effects of tetracaine on charge movement in fast twitch rat skeletal muscle fibers. *J. Physiol.* 421:633–644.

Holmberg, S.R.M., and A.J. Williams. 1990. Patterns of interaction between anthraquinone drugs and the calcium-release channel from sarcoplasmic reticulum. *Circ. Res.* 67:272–283.

Horowicz, P., and M.F. Schneider, 1981. Membrane charge moved at contraction thresholds in skeletal muscle fibres. *J. Physiol.* 314: 595–633.

Huang, C.L.-H. 1981*a*. Dielectric components of charge movements in skeletal muscle. *J. Physiol.* 313:187–205.

Huang, C.L.-H. 1981*b*. Membrane capacitance in hyperpolarized muscle fibers. *J. Physiol.* 313:207–222.

Huang, C.L.-H. 1982. Pharmacological separation of charge movement components in frog skeletal muscle. *J. Physiol.* 324:375–387.

Huang, C.L.-H. 1983. Time domain spectroscopy of the non-linear capacitance in frog skeletal muscle. *J. Physiol.* 341:1–24.

Huang, C.L.-H. 1984. Analysis of "off" tails of intramembrane charge movements in skeletal muscle of Rana temporaria. *J. Physiol.* 356:375–390.

Huang, C.L.-H. 1990. Voltage-dependent block of charge movement components by nifedipine in frog skeletal muscle. *J. Gen. Physiol.* 96:535–558.

Huang, C.L.-H. 1993. Intramembrane Charge Movements in Striated Muscle. Monographs of the Physiological Society. No. 44. Clarendon Press, Oxford. 292 pp.

Huang, C.L.-H. 1994*a*. Charge conservation in intact frog skeletal muscle fibres in gluconate-containing solutions. *J. Physiol.* 474: 161–171.

Huang, C.L.-H. 1994*b*. Kinetic separation of charge movement components in intact amphibian skeletal muscle. *J. Physiol.* 481: 357–369.

Huang, C.L.-H., and L.D. Peachey. 1989. The anatomical distribution of voltage-dependent membrane capacitance in frog skeletal muscle fibers. *J. Gen. Physiol.* 93:565–584.

Hui, C.S. 1983. Differential properties of two charge components in frog skeletal muscle. *J. Physiol.* 337:531–552.

Hui, C.S. 1994. A component of charge movement temporally coupled to the calcium release signal. *Biophys. J.* 66:A340 (Abstr.)

Hui, C.S., and W.K. Chandler. 1990. Intramembranous charge movement in frog cut twitch fibers mounted in a double vaseline-gap chamber. *J. Gen. Physiol.* 96:257–297.

Hui, C.S., and W.K. Chandler. 1991. Q_β and Q_γ of intramembranous charge movements in frog cut twitch fibers. *J. Gen. Physiol.* 98:429–464.

Hui, C.S., and W. Chen. 1992. Separation of Q_β and Q_γ charge components in cut twitch fibers with tetracaine. Critical comparison with other methods. *J. Gen. Physiol.* 99:985–1016.

Jong, D.S., P.C. Pape, and W.K. Chandler. 1995. Effect of sarcoplasmic reticulum calcium depletion on intramembranous charge movement in frog cut muscle fibers. *J. Gen. Physiol.* 106:659–704.

Kostyuk, P.G., O.A. Kristal, and V.I. Pidoplichko. 1981. Calcium inward current and related charge movements in the membrane of snail neurones. *J. Physiol.* 310:403–421.

Kovacs, L., E. Rios, and M.F. Schneider. 1979. Calcium transients and intramembrane charge movements in skeletal muscle fibres. *Nature (Lond.).* 279:391–396.

Lamb, G.D. 1986. Components of charge movement in rabbit skeletal muscle: The effect of tetracaine and nifedipine. *J. Physiol.* 376:85–100.

Lopez-Lopez, J., P.S. Shacklock, C.W. Balke, and W.G. Wier. 1995. Local calcium transients triggered by single L-type calcium channel currents in cardiac cells. *Science (Wash. DC).* 268:1042–1045.

Meissner, G. 1994. Ryanodine receptor/Ca^{2+} release channels and their regulation by endogenous effectors. *Annu. Rev. Physiol.* 56: 485–508.

Melzer, W., M.F. Schneider, B.J. Simon, and G. Szucs. 1986. Intramembrane charge movement and calcium release in frog skeletal muscle. *J. Physiol.* 373:481–511.

Olivares, E.B., S.J. Tanksley, J.A. Airey, C.F. Beck, Y. Ouyang, T.J. Deerink, M.H. Ellisman, and J.L. Sutko. 1991. Nonmammalian vertebrate skeletal mucles express two triad junctional foot protein isoforms. *Biophys. J.* 59:1153–1163.

Pape, P.C., D.S. Jong, and W.K. Chandler. 1996. A slow component of intramembranous charge movement during sarcoplasmic reticulum calcium release in frog cut muscle fibers. *J. Gen. Physiol.* 107:79–101.

Peachey, L.D. 1965. The sarcoplasmic reticulum and transverse tubules of the frog's sartorius. *J. Cell Biol.* 25:209–231.

Pessah, I.N., E.L. Durie, M.J. Schiedt, and I. Zimanyi. 1990. Anthraquinone-sensitized Ca^{2+} release channel from rat cardiac sarcoplasmic reticulum: Possible receptor-mediated mechanism of doxorubicin cardiomyopathy. *Mol. Pharmacol.* 37:503–514.

Pizarro, G., L. Csernoch, I. Uribe, M. Rodriguez, and E. Rios, 1991. Ther relationship between Q_γ and Ca release from the sarcoplasmic reticulum in skeletal muscle. *J. Gen. Physiol.* 97:913–947.

Polakova, K., and J.A. Heiny. 1994. Effects of intracellular Ca^{2+} on charge movement in frog skeletal muscle. *Biophys. J.* 66:A86 (Abstr.)

Press, W.H., B.P. Flanney, S.A. Teukolsky, and W.T. Vetterling. 1986. Modeling of data. *In* Numerical Recipes. The Art of Scientific Computing. Cambridge University Press, Cambridge. 523–528.

Rakowski, R.F., P.M. Best, and M.R. James-Kracke. 1985. Voltage-dependence of membrane charge movement and calcium release in frog skeletal muscle fibers. *J. Muscle Res. Cell Motil.* 6:403–433.

Rios, E., M. Karhanek, J. Ma, and A. Gonzalez. 1993. An allosteric model of the molecular interactions of excitation-contraction coupling in skeletal muscle. *J. Gen. Physiol.* 102:449–481.

Rios, E., and G. Brum. 1987. Involvement of dihydropyridine receptors in excitation-contraction coupling. *Nature (Lond.).* 325:717–720.

Rouseau, E.J., S. Smith, and G. Meissner. 1987. Ryanodine modifies conductance and gating behavior of single Ca^{2+} release channel. *Am. J. Physiol.* 253:C364–C368.

Scheuer, T., and W.F. Gilly. 1986. Charge movement and depolarization-contraction coupling in arthropod vs vertebrate skeletal muscle. *Proc. Natl. Acad. Sci. USA.* 83:8799–8803.

Schneider, M.F., and W.K. Chandler. 1973. Voltage-dependent charge in skeletal muscle: A possible step in excitation-contraction coupling. *Nature (Lond.).* 342:244–246.

Shirokova, N., G. Pizarro, and E. Rios. 1991. A damped oscillation

of the intramembranous charge movement and calcium release flux of frog skeletal muscle fibers. *J. Gen. Physiol.* 104:449–477.

Simon, B.J., and D. Hill. 1992. Charge movement and SR calcium release in frog skeletal muscle can be related by a Hodgkin-Huxley model with four gating particles. *Biophys. J.* 61:1109–1116.

Simon, B.J., and K.G. Beam. 1985. Slow charge in mammalian skeletal muscle. *J. Gen. Physiol.* 85:1–19.

Sugiyama, K., and T. Muteki. 1994. Local anaesthetics depress the calcium current of rat sensory neurons in culture. *Anesthesiology.* 80:1369.

Sun, X.H., F. Protasi, M. Takahashi, H. Takeshima, D.G. Ferguson, and C. Franzini-Armstrong. 1995. Molecular architecture of membranes involved in excitation-contraction coupling of cardiac muscle. *J. Cell Biol.* 129:659–671.

Szucs, G., L. Csernoch, J. Magyar, and L. Kovacs. 1991. Contraction threshold and the "hump" component of charge movement in frog skeletal muscle. *J. Gen. Physiol.* 97:897–911.

Takekura, H., L. Bennett, T. Tanabe, K.G. Beam, and C. Franzini-Armstrong. 1994. Restoration of junctional tetrads in dysgenic myotubes by dihydropyridine receptor cDNA. *Biophys. J.* 67:793–803.

Takekura, H., N. Nishi, T. Noda, H. Takeshima, and C. Franzini-Armstrong. 1995. Abnormal junctions between surface membranes and sarcoplasmic reticulum in skeletal muscle with a mutation targetted to the ryanodine receptor. *Proc. Natl. Acad. Sci. USA.* 92:3381–3385.

Vergara, J., and C. Caputo. 1982. Effects of tetracaine on charge movements and calcium signals in frog skeletal muscle fibers. *Proc. Natl. Acad. Sci. USA.* 80:1477–1481.

Zimanyi, I., E. Buck, J.J. Abramson, M.M. Mack, and I.N. Pessah. 1992. Ryanodine induces persistent inactivation of the Ca^{2+} release channel from skeletal muscle sarcoplasmic reticulum. *Mol. Pharmacol.* 42:1049–1057.